NTIA-Report-80-40

Fading Statistics on a 23 km Link at 9.6 and 28.8 GHz

R. H. Ott
K. C. Allen
E. J. Violette
R. H. Espeland
M. C. Thompson, Jr.
A. R. Mitz

U.S. DEPARTMENT OF COMMERCE
Philip M. Klutznick, Secretary

Henry Geller, Assistant Secretary
for Communications and Information

June 1980

TABLE OF CONTENTS

LIST OF FIGURES

FADING STATISTICS ON A 23 km LINK AT 9.6 AND 28.8 GHz

R. H. Ott, K. C. Allen*, E. J. Violette, R. H. Espeland,
M. C. Thompson, Jr., and A. R. Mitz

An experimental study of atmospheric multipath on a 23 km link at 9.6 and 28.8 GHz near Boulder, Colorado, is described. The preliminary observations were made for three days in July 1979 when a strong inversion layer was present, creating an elevated tropospheric duct. The possible influence of antenna aperture size on atmospheric multipath was investigated by observing fades and enhancements on the 28.8 GHz carrier using a 10° horn and a 1.2° parabolic dish. Continuous height-gain observations were obtained using the 300 m. tower at Erie, Colorado, as one end of the link. Meteorological data at the tower were also recorded during observation periods of the radio signal.

Key Words: atmospheric multipath, fading, micro-millimeter wave, refractivity structure

1. INTRODUCTION

Present interest in using high-speed digital transmission of information has precipitated the need for understanding the mechanisms responsible for fading. This paper describes initial fading data on a 22.8 km link from the Boulder Atmospheric Observatory (BAO) at Erie, Colorado, to the U. S. Department of Commerce Radio Building in Boulder, Colorado.

In order to characterize a radio channel, which has known coherent bandwidth properties for no multipath, the amplitude and delay of each of the multipath components needs to be measured. Techniques for estimating the parameters in a channel characterized by three paths or rays have been described in the literature. One technique requires several thousand scans of the power spectrum. Each scan consists of a power measurement at each of several frequencies separated sufficiently to define the passband and at the same time of sufficient number to define the characteristics of the channel within the passband. It appears that Rummler's method is well suited for investigating the multipath phenomena produced by three-ray fades. Unfortunately, instrumentation for making the power scans required was not available at the time these observations were being performed.

*Boulder Experimental Studies Institute, Boulder, Colorado 80302.
The rest of the authors are with the U. S. Department of Commerce, National Telecommunications and Information Administration, Institute for Telecommunication Sciences, Boulder, Colorado 80303.

However; spatial and temporal observations of fades at two harmonically related frequencies, did show interesting lobing, characteristic of multipath. We hope to convince the reader this lobing resulted from two or more rays reaching the receiver without suffering ground reflections; i.e., purely atmospheric multipath. We claim that the observed multipath was caused by trapping of the radio energy within an elevated duct in the atmosphere formed by an inversion layer. We will try to support this assertion on the basis of fading data from three days in late July, 1979. The preliminary results presented in this report suggest that the unique measurement facility may contribute towards the understanding of atmospheric multipath and testing of the 3-ray model.

2. MEASUREMENT FACILITY

The BAO tower at Erie, located 25 km east of the Rockies on gently rolling terrain, is a unique facility for calibrating meteorological instruments and remote sensors and for studying the planetary boundary layer. The BAO is operated by the Wave Propagation Laboratory (WPL) of the National Oceanic and Atmospheric Administration (NOAA), U. S. Department of Commerce.

The central feature of the BAO is a 300 m tower. It is instrumented at eight fixed levels with fast-response anemometry and thermometry for measuring both turbulent and mean properties of the boundary-layer airflow. Instruments on each level also provide humidity information. A two-man elevator inside the tower provides access to the fixed instrumentation levels. A movable carriage on the tower's southwest face, able to carry up to 1000 kg of equipment, permits continuous profiling or fixed-level operation at any desired height.

Acoustic echo sounders, optical anemometry, and an array of sensitive microbarographs complete the standard instrumentation (cf. Figure 1). A computer in a van at the base of the tower now handles the data acquisition. A calibration facility consisting of a small wind tunnel and constant-temperature bath is also available.

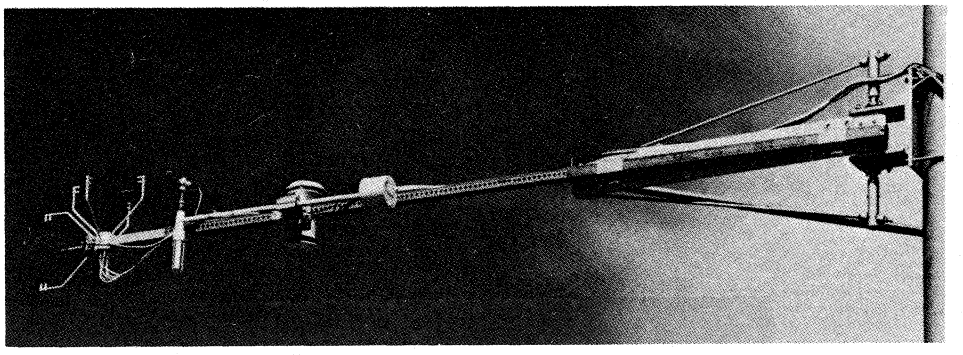

Figure 1. Instrumentation at BAO tower. At each level, three-axis sonic anemometers measure mean and turbulent wind components. A fine platinum wire thermometer attached to the vertical velocity probe measures the fluctuating temperature. Mean temperature is measured by a quartz thermometer in an aspirated shield; dewpoint temperature is monitored by a cooled mirror hygrometer.

The path profile for the BAO-Radio Building path is shown in Figure 2. A unique feature of the path is that even under conditions where atmospheric refraction may cause a ground-reflected component, this ray component may be blocked from reaching the antenna at the Radio Building because of the knife-edge-like obstruction at Hoover Hill. We will try to support this statement with observed data later in the report.

Frequencies of 9.6 and 28.8 GHz were investigated. The approach was to use a 100 MHz Voltage Controlled Crystal Oscillator (VCXO) to drive a multiplier-amplifier to provide 11.4 mW (10.6 dBm) at 9.6 GHz. This signal was multiplied by three and used to injection lock Varian Gunn effect diode source that provided 83 mW (19.2 dBm) at 28.8 GHz.

The two transmit antennas, located on the tower at Erie, were a parabolic dish at 9.6 GHz having a 3-dB beamwidth of 4.8° and a horn at 28.8 GHz having a 3-dB beamwidth of 10°. The three receive antennas, located on the roof of wing 4 of the Radio Building at Boulder, were a parabolic dish at 9.6 GHz having a 3-dB beamwidth of 1.7° and two antennas at 28.8 GHz, one parabolic dish having a 3-dB beamwidth of 1.2° and a horn having a 3-dB beamwidth of 10°. The two receive antennas were used at 28.8 GHz to investigate the effect of antenna beamwidth on multipath fading.

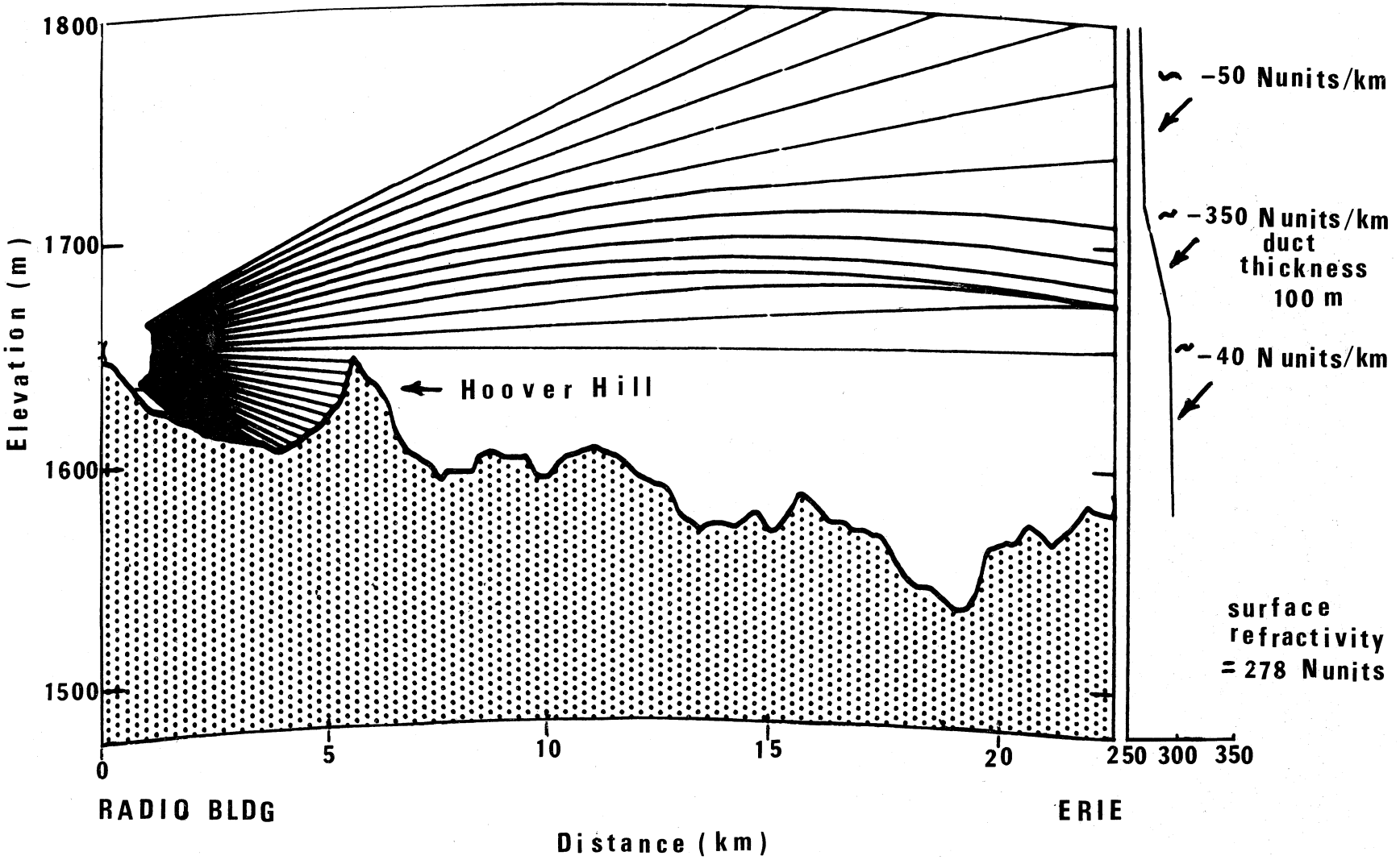

Figure 2. Path profile for link between Erie and Radio Building. The profile is drawn using a true earth radius with a vertical exaggeration of 50 to 1. The plot on the right shows one sample of the observed refractive index profile at 0900 MDT, 26 July, 1979. Also shown is a ray trace using the refractive index profile shown, and focusing at about 100 m above the ground at Erie.

A link power budget is given by

$$P_R = 10 \log_{10} P_t + G_T + G_R - 20 \log_{10} d(km) - 20 \log_{10} f(MHz) - L_A - L_T - L_R - 32.45 \quad (1)$$

where

L_A = loss due to water vapor absorption (dB) (5% relative humidity)

L_T = transmission line loss at transmitter (dB)

L_R = transmission line loss at receiver (dB)

P_t = transmitted power (mW)

G_T = transmitting antenna gain (dB)

G_R = receiving antenna gain (dB)

d = path distance (km)

f = frequency (MHz).

The last term of equation (1) is the constant resulting from the units for kilometers and megahertz and is given by $10 \log_{10}(3 \times 10^5$ km/sec$/16\pi^2 \times 10^6$ MHz$) = -32.45$

At 9.6 GHz (1) gives

$$P_R(dBm) \cong 10.6 + 30.0 + 38.6 - 27.2 - 79.6 - 0.2 - 0.5 - 0.5 - 32.45 \cong -61.2$$

At 28.8 GHz (1) gives for the parabolic receiving antenna

$$P_R(dBm) \cong 19.2 + 26.2 + 42.1 - 27.2 - 89.2 - 0.4 - 2 - 2 - 32.45 \cong -65.7$$

At 28.8 GHz (1) gives for the horn receiving antenna

$$P_R(dBm) \cong 19.2 + 26.2 + 26.2 - 27.2 - 89.2 - 0.4 - 2 - 2 - 32.45 \cong -81.6$$

The signal-to-noise ratio (S/N) of the receiver, is determined by the first stage rf mixer, and is given by

$$S/N = P_R(dBw) - \text{mixer conversion loss (dB)} - 10 \log_{10}(kTB) \quad (2)$$

where

$T = (N_F - 1)\ 290°K$

$k = 1.38 \times 10^{-23}$ joules/degree

and N_F is the noise figure of the mixer. The bandwidth, B, was 2 kHz. At 9.6 GHz, N_F = 10 dB and (2) gives

$$S/N \cong -91.2 -10 + 161.4$$
$$\cong 60 \text{ dB}.$$

At 28.8 GHz, B was 5 kHz and N_F was 6 dB (Note, normally the noise figure would be higher at the higher frequency, however, the quality of the mixer was much better at 28.8 GHz than 9.6 GHz). For the parabolic receiving antenna (2) gives

$$S/N \cong -95.7 -6 + 162.2$$
$$\cong 60.5 \text{ dB}$$

and for the horn antenna at 28.8 GHz (2) gives

$$S/N \cong -111.6 -6 + 162.2$$
$$\cong 44.6 \text{ dB}$$

3. MULTIPATH FADING MECHANISMS

In this section some background is given on the various meteorological mechanisms affecting a radio wave. Much of the discussion in this section is given in a report by Hufford et al. (1975 OT Tech. Memo 75-196, Radio propagation to the offshore extended area, limited distribution) together with many examples. The number of references that deal with this subject is so large we will not even begin to try to list them all. We will, however, give in the bibliography some indication of those papers and reports that have been helpful during this investigation. Under so-called "standard" conditions the atmosphere is turbulent, well-mixed, and its refractive index decreases rather uniformly with height above the earth's surface. However, under certain meteorological conditions, layers are formed in the atmosphere producing gradients in the refractive index profile as a function of height. These layers may be caused by differences in temperature or water vapor content. This gives rise to the phenomena of multipath and radio holes.

When strong superrefraction occurs in an atmospheric layer, radio waves are "trapped" or guided along the layer and the layer is referred to as an atmospheric duct. The signal fading under such circumstances is strongly dependent on the heights of the transmitter and receiver.

When the atmospheric conditions produce reflections from an elevated layer or when ground-reflections are present two or more rays may reach the receiving terminal and interfere constructively or destructively. In these cases the radiation pattern of the receiving antenna together with its height and pointing may play a critical role in the level of the received signal. The effect of antenna aperture on atmospheric-induced ground-reflected multipath is illustrated in Figure 3.

If the transmitter is above an atmospheric layer, a "radio hole" may be observed. This phenomenon is a diffraction interference mechanism much like knife-edge diffraction. Figure 4 shows an illustration of a radio hole (from Hufford et al.) The importance of layers in this paper leads us to adopt definitions of descriptive terms for layer intensity as given in Table I.

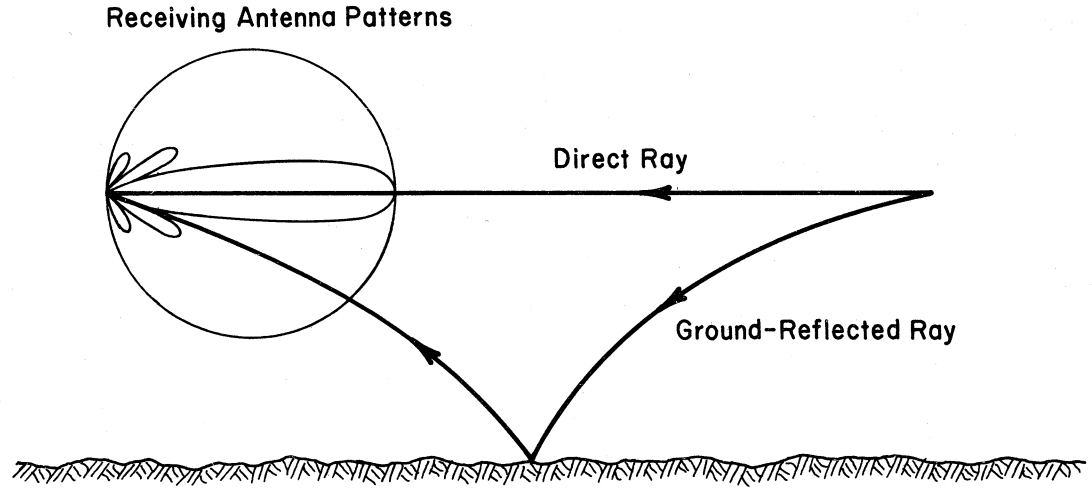

Figure 3. Effect of antenna size or gain on ground-reflected, atmospheric induced multipath.

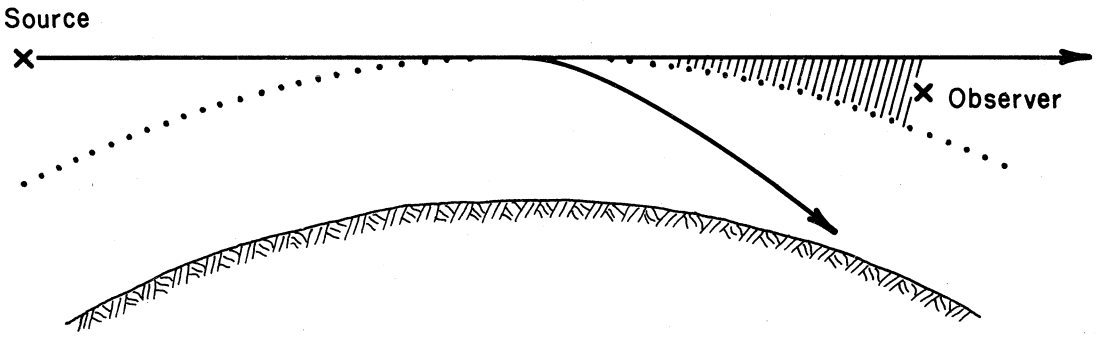

Figure 4. The classical radio hole. The dotted curve defines the top of a ducting layer. No signal reaches an observer in the shaded region.

TABLE I

Descriptive terms for layer intensity (from Hufford et al.)

Descriptive Term	Vertical Gradient of Refractivity N-units/km
Subrefractive	> 0
Normal	- 40
Superrefractive	< - 80
Ducting	< -157
Extreme ducting	< -314

4. GROUND REFLECTIONS AND ATMOSPHERIC MULTIPATH

We will use the term "diffraction interference" in this report to include the fades observed in radio holes as well as the enhancements observed near ray caustics. The lobing of the signal when observing atmospheric multipath can be caused by two or more rays interferring constructively or destructively or by a radio hole where the ray density becomes small and the variation in field strength appears like classical knife-edge diffraction. Figure 5 shows the path profile and the lower half of the first Fresnel ellipse such that the ellipse just grazes the ridge assuming an effective earth's radius of 4/3. For the geometry in Figure 5, the contribution from the direct ray is 180° out of phase with the ray reflected from the top of the ridge where the ellipse grazes the ridge. As the transmitter at the BAO tower is lowered so that the line-of-sight (direct) ray just grazes the ridge, the received signal will drop 6 dB below the free-space value.

Also shown in Figure 5 are the 3-dB beamwidths for the transmitting and receiving parabolic antennas. The transmitting and receiving horn antennas illuminate practically all the ground between the transmitter and receiver's terminals. However, Hoover Hill, in Figure 5 must prohibit some ground reflected paths from reaching the receiving antenna.

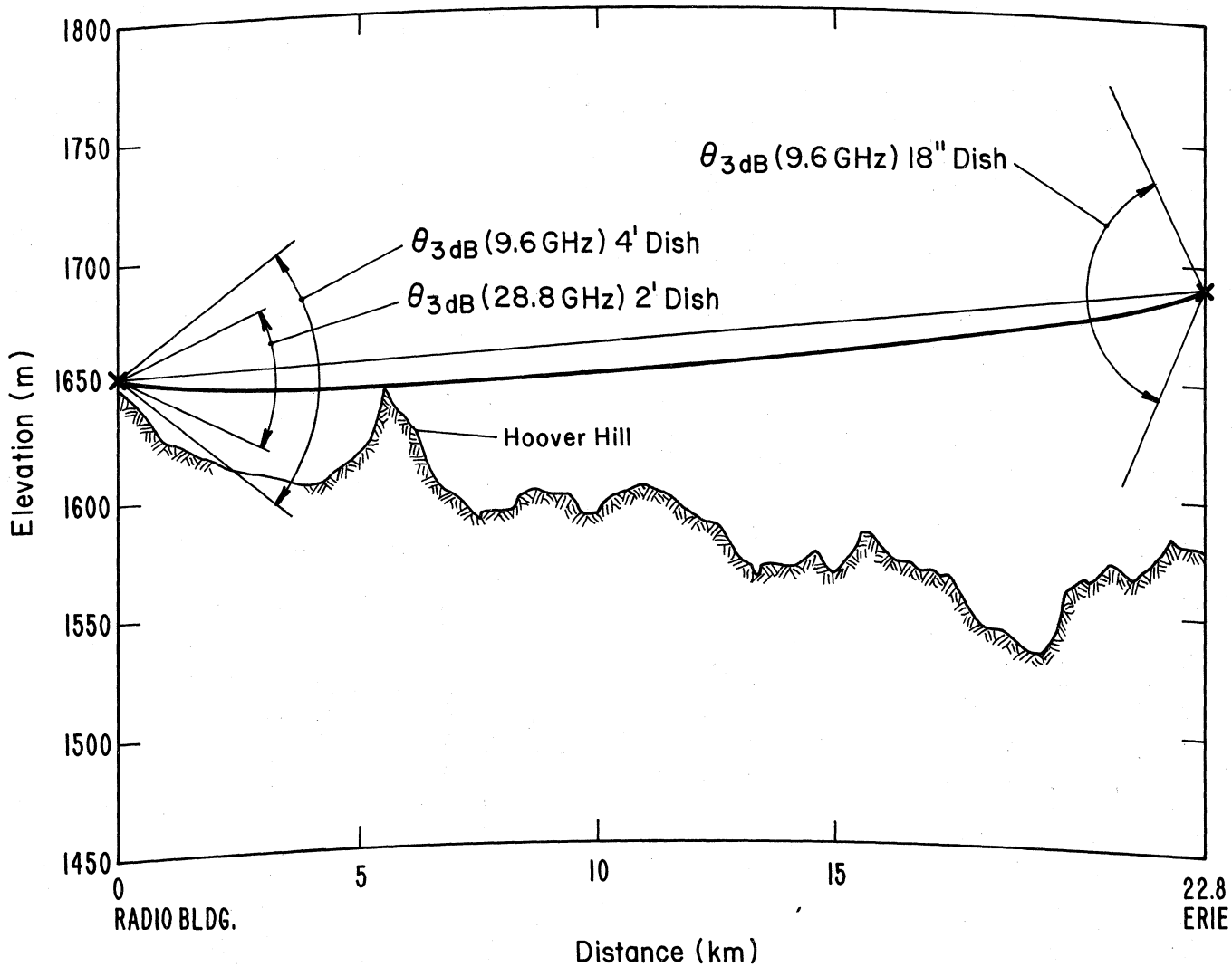

Figure 5. The first Fresnel ellipse that just grazes the ridge occurs for a transmitting antenna height of 110 m, 9.6 GHz and a 4/3 earth's radius. 3-dB beamwidths for parabolic transmitting and receiving antennas also shown.

5. MULTIPATH OBSERVATIONS

Along with the three components of the wind, the BAO tower has provisions for measuring the temperature and dew point temperature at the heights 10, 20, 50, 100, 150, 200, 250, and 300 m above the ground. One- or ten-minute samples are available. Using the observed refractivity structure at 0900 MDT, July 26, 1979, Figure 2 shows a ray trace from the Radio Building to Erie. Remember, the transmitter was actually at Erie so the reader should think of placing the transmitter about 100 m above the ground at the BAO tower (i.e., where the rays coalesce) for the unobstructed direct ray to reach the receiver. The refractivity structure shown in Figure 2 corresponds to a 10-minute sample. The time required to make an ascent and descent was about 6 minutes. The temporal stability of the refractive index structure during these height gain runs was checked by sampling the temperature and dew point temperatures at five 1-minute intervals and the results were nearly identical to the 10-minute samples. The gradient in Figure 2 of -350 N-units/km is well within the definition of an "extreme duct" in Table I. The refractivity structure at mid-path may be different than at the BAO tower. Although information on refractivity structure was not available at other points along the path layering tends to be somewhat uniform over a region of this size, and this assumption will be made for the purpose of this paper. In the fading data which follows it may help the reader to recall the ray trace in Figure 2 showing the possibility of caustics or radio holes.

Fading data is presented in two forms: 1) time series for the received signal with the carriage at the BAO tower at a fixed height of 217 m and 2) height-gain runs. Explanations for the fades or enhancements are only conjectures at this point and much more research is required before one can explain all the features in a particular observed signal. An additional word of caution concerns the range of fades with the tower at a fixed height. Our observations show fades in the 5- to 10-dB range. These are probably associated with the random motions of the atmosphere caused by turbulent eddies on the top or bottom side of the tropospheric duct. They are not of the 20-dB variety that cause severe outages in millimeter wave links. Large fades at 25-30 dB were observed on the height-gain runs.

Figure 6 shows time series for the received 9.6 GHz, 28.8 GHz horn and 28.8 GHz dish signals starting at 1010 and ending at 1036, July 26, 1979, with the carriage at a fixed height of 217 m. The greatest variability (i.e., about 8 dB) in the signal occurred between 1025 and 1035.

In Figures 7a and 7b we show the scatter plot for this time period. In Figures 6 and 7, the received signals have an absolute calibration; i.e., 0-dB corresponds to the free-space signal strength. It is rather curious that the 28.8 GHz horn signal never reached the free-space value while the 28.8 GHz dish signal did. This is opposite to what one would normally expect taking into consideration the respective beamwidths. In Figure 7a, the correlation between the 28.8 GHz horn and dish signals is 0.58. Therefore about one-third the variance in the 28.8 GHz horn signal is associated with the 28.8 GHz dish signal. Also, in Figure 7a, the received signals are seen to be clustered into two sets. In order to study this effect in more detail, we divided the two clusters in Figure 7a as shown in Figure 8. The two clusters in Figure 8 represent unexpected results from a fading mechanism. The time series corresponding to Figure 8 is replotted in Figure 9 where the cluster above the line in Figure 8 is shown as a heavy trace and the one below the line as a light trace. The dish signal in Figure 9 seemed to remain at a constant level (aside from scintillations about the mean) while the horn signal increased at about 1025. The division into two clusters was caused by a relatively long term signal variation while the scatter (scintillation) within each cluster was caused by the short term signal variation. This would point to two different mechanisms being present. For example turbulence plus ducting.

Recently, much of the concern with multipath degradation has focused on a 3-ray model. Analysis of Bell Telephone Laboratory data has shown that two of the paths have an extremely small delay (i.e., a small fraction of a bit duration but comparable with the period of the carrier frequency) but tend to cancel each other leaving a signal level determined by a third ray with a relatively long delay (i.e., comparable with the bit duration or several bit durations). A 3-ray model for multipath is

$$r(t) = 1 + a_1(t)\exp[i\theta_1(t)] + a_2(t)\exp[i\theta_2(t)], \qquad (3)$$

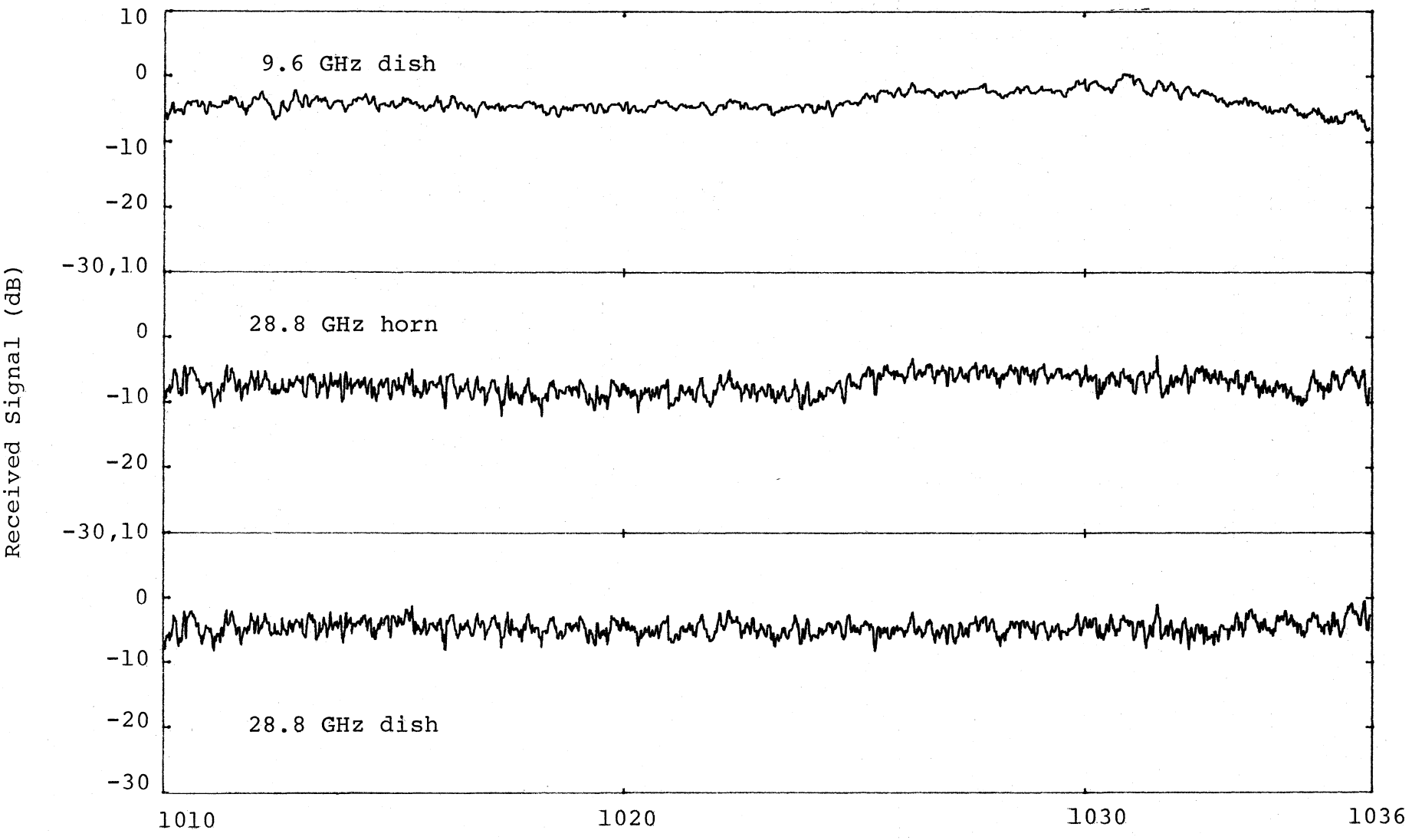

Figure 6. Time series for 9.6 GHz, 28.8 GHz horn, 28.8 GHz dish starting at 1010 and ending at 1036, July 26, 1979. Carriage at 217 m. E{9.6 GHz} ≃ -2.67 dB, E{28.8 GHz dish} ≃ -9.06 dB, E{28.8 GHz horn} ≃ -10.262 dB, σ^2(9.6 GHz) ≃ 1.93 dB^2 , σ^2(28.8 GHz dish) ≃ 25.76 dB^2 , σ^2(28.8 GHz horn) ≃ 23.19 dB^2. 0-dB corresponds to free space.

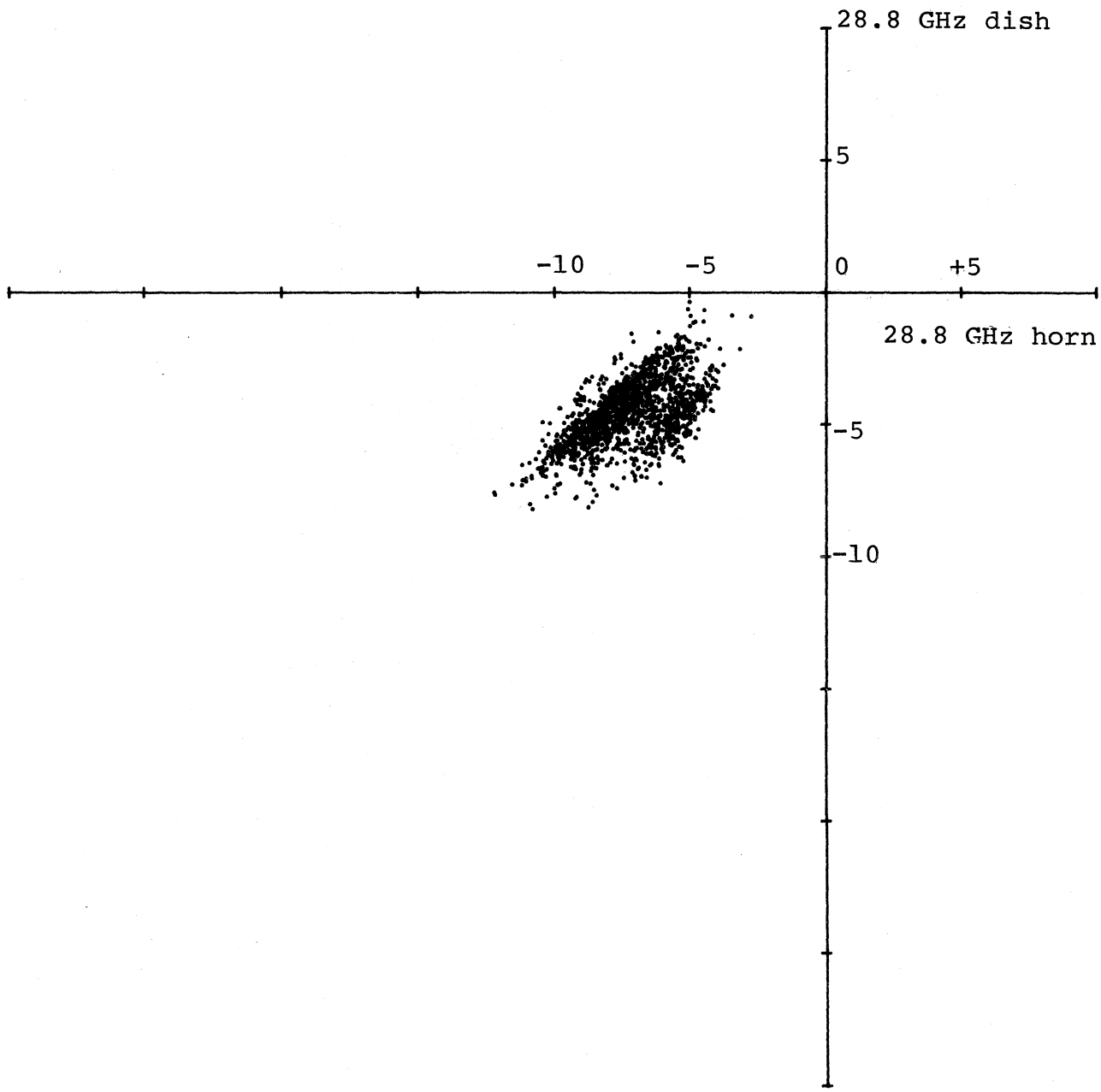

Figure 7a. Scatter plot for 28.8 GHz horn and dish signals on July 26, 1979, corresponding to time series in Figure 6. The origin corresponds to free space.

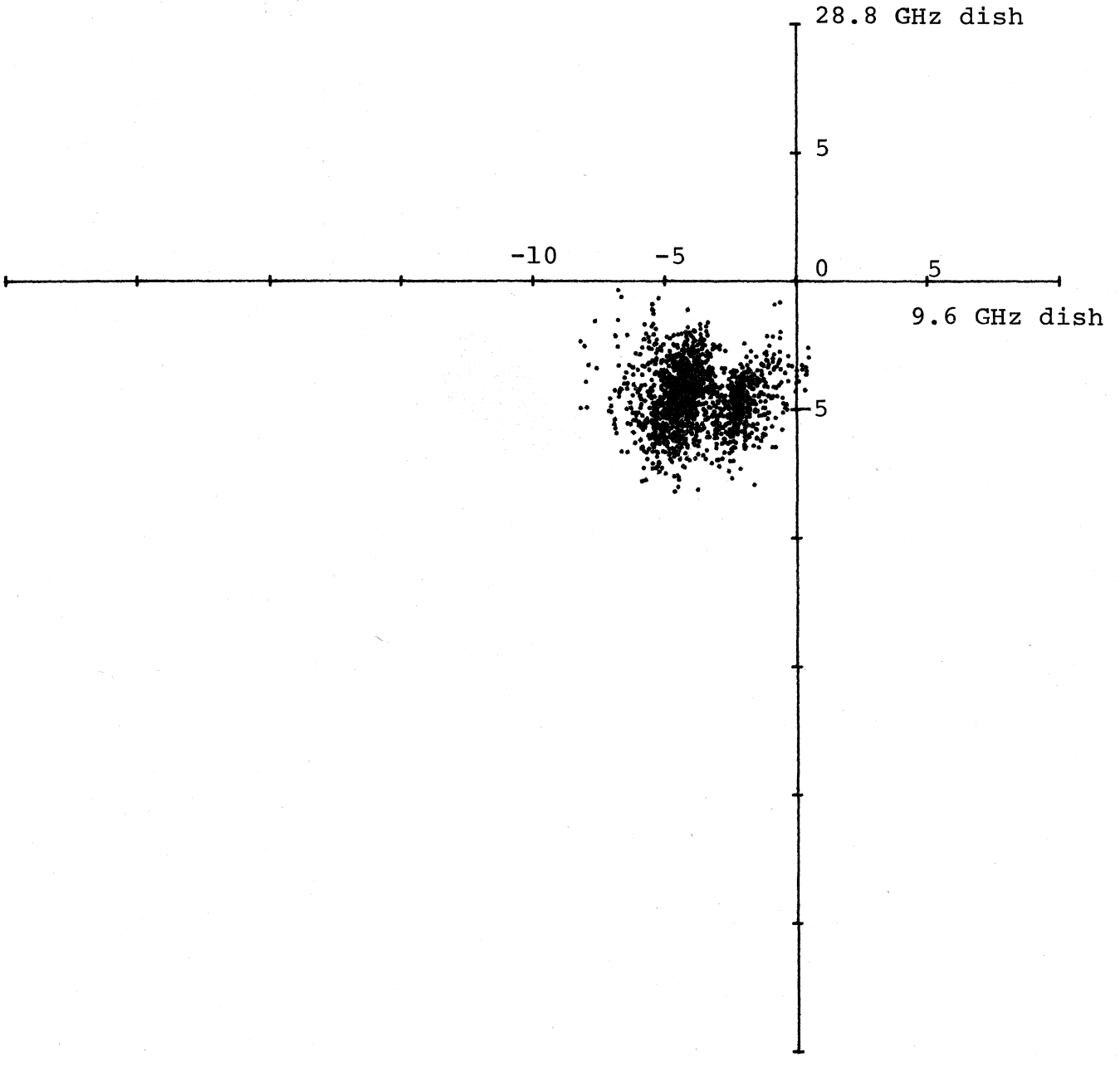

Figure 7b. Scatter plot for 9.6 GHz dish and 28.8 GHz dish signals on July 26, 1979 corresponding to time series in Figure 6. The origin corresponds to free space.

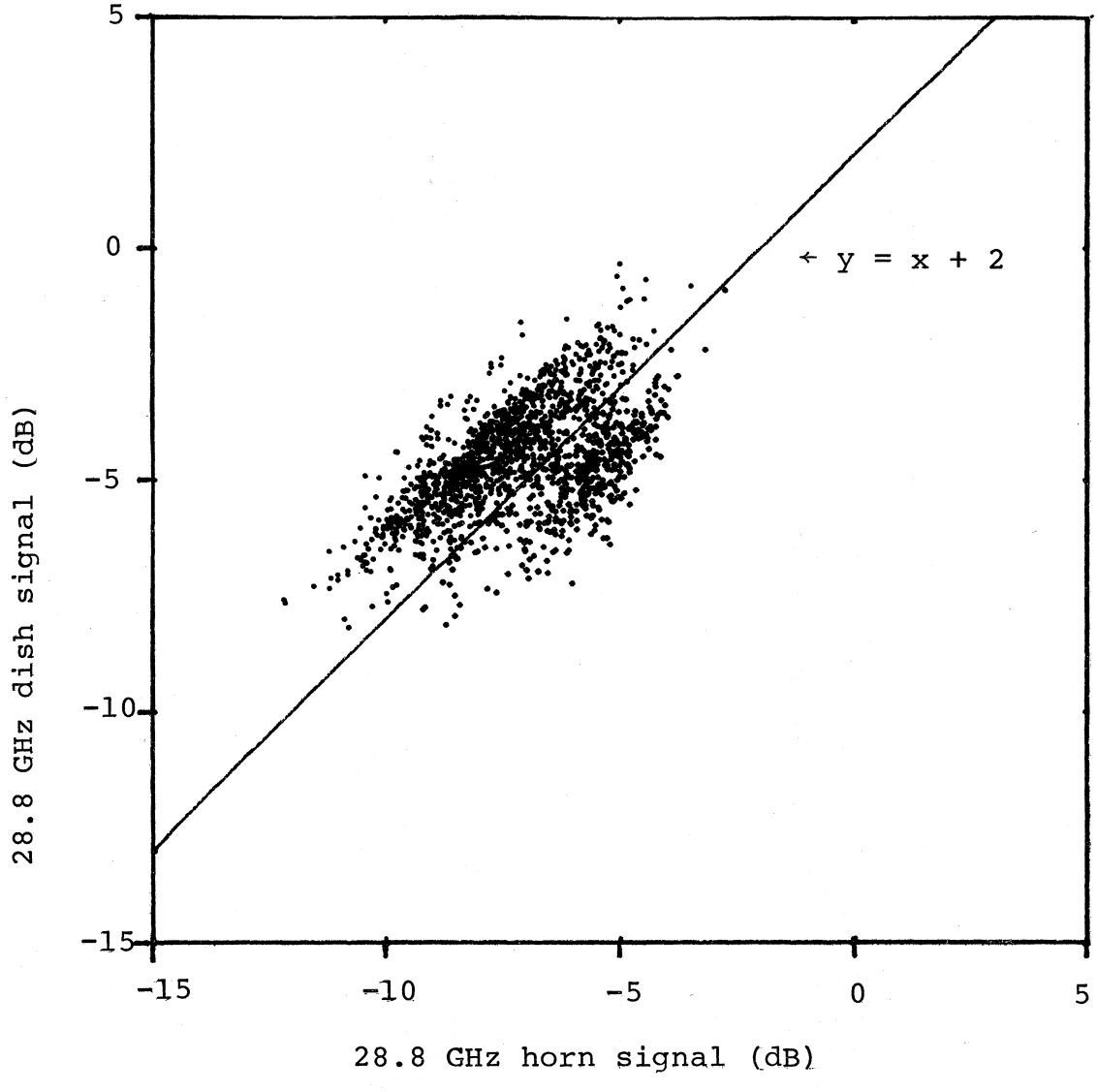

Figure 8. Scatter plot for the 28.8 GHz horn and dish signals for a subset of the time period shown in Figure 7a. The scatter plot is shown divided into two clusters, to test a hypothesis.

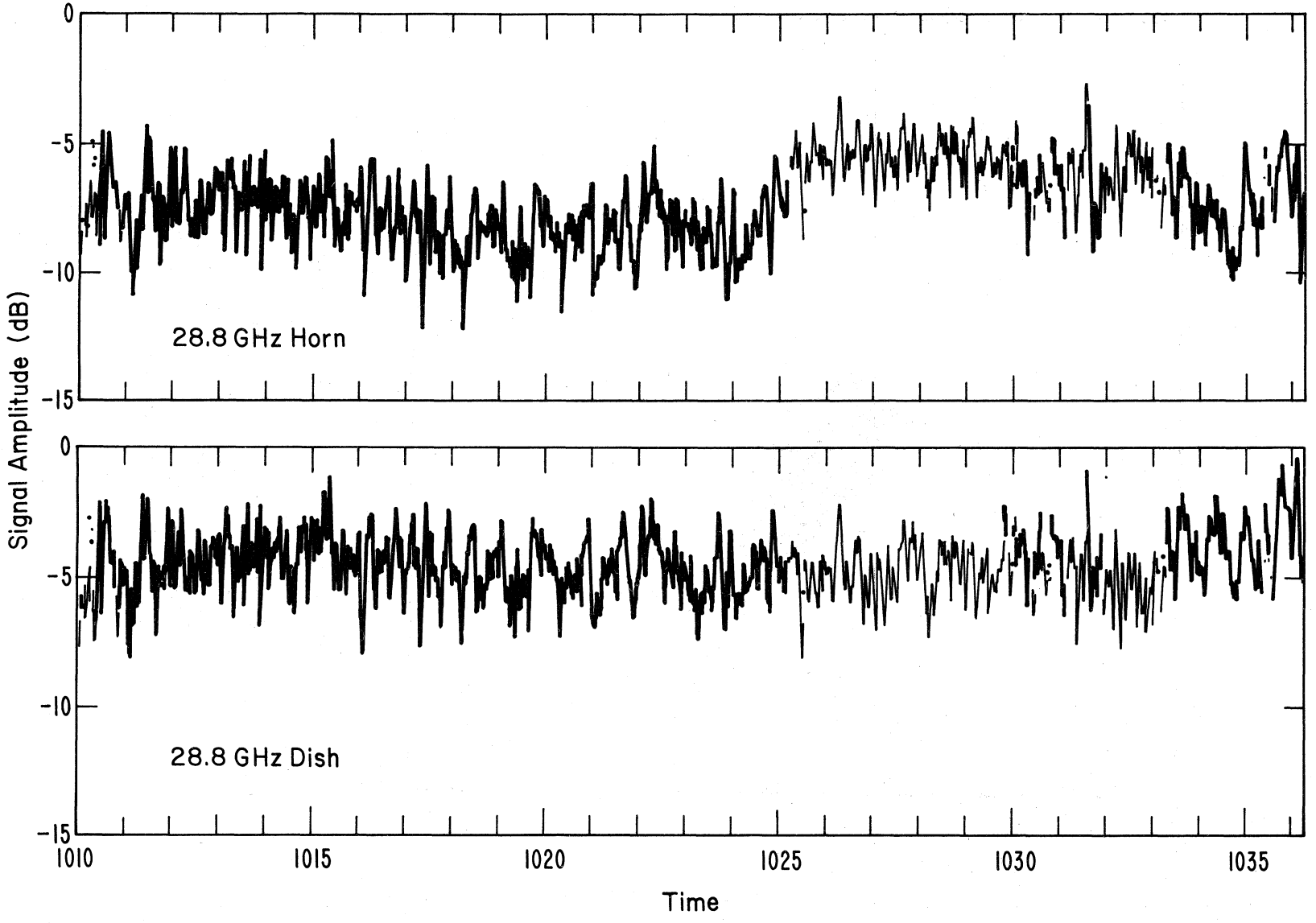

Figure 9. Time series for the 28.8 GHz horn and dish signals in Figure 8 assuming two clusters of points.

where r(t) is the received signal. When the signal is in the state or cluster above the line in Figure 8, we hypothesize the 2nd two multipath rays in (3) cancel and the horn and dish see the same signal. When the signal is in the state or cluster below the line in Figure 8, we hypothesize that the 3rd multipath component in (3); i.e., a_2 arrives at an angle outside the 3-dB beamwidth of the 28.8 GHz dish but within the 3-dB beamwidth of the 28.8 GHz horn antenna. Since the 28.8 GHz dish signal in Figure 9 did not change state, we assume that the 2nd multipath component in (3); i.e., a_1 is small. The quantities θ_1 and θ_2 in (3) are the path differences between the direct and 2nd and 3rd multipath components and their variation may be small compared to the electrical wavelength, which in our example is approximately 1 cm. This may explain why the signal remains in a particular state for relatively long periods of time. The model in (3) also covers the possible case where a_1 and a_2 are nearly equal in magnitude and θ_1 and θ_2 are 180° out of phase; and in addition, the dish could receive the direct plus 2nd multipath component but not the 3rd multipath component. This set of circumstances would cause the 28.8 GHz dish signal to drop in going from one state to the next while the 28.8 GHz horn signal would remain constant. The 3-ray model for atmospheric multipath does not account for diffraction effects associated with radio holes or antiholes. Diffraction effects need to be examined using a full wave type of solution (Hufford, et al., 1975).

In Figure 10 we show height-gain runs for the received signals as the carriage made ascents and descents on the BAO tower from 0722 MST to 0737 MST, July 26, 1979. The signals in Figure 10 have an absolute calibration; i.e., 0 dB corresponds to the free-space signal level. The time for an ascent or descent was about 6 min. The velocity of the carriage is about 0.58 m/sec. The height-gain runs for ascent and descent in Figure 10 are offset 20 dB from one another for clarity. First Fresnel zone clearance at Hoover Hill occurs with the carriage about 110 m above the ground. The enhancements in the fields as the carriage passed through this height can be seen in Figure 10. The field 6 dB down from its free-space value gives the location of optical grazing which is about 90 m above the ground. Figure 11 shows the first Fresnel zone with the

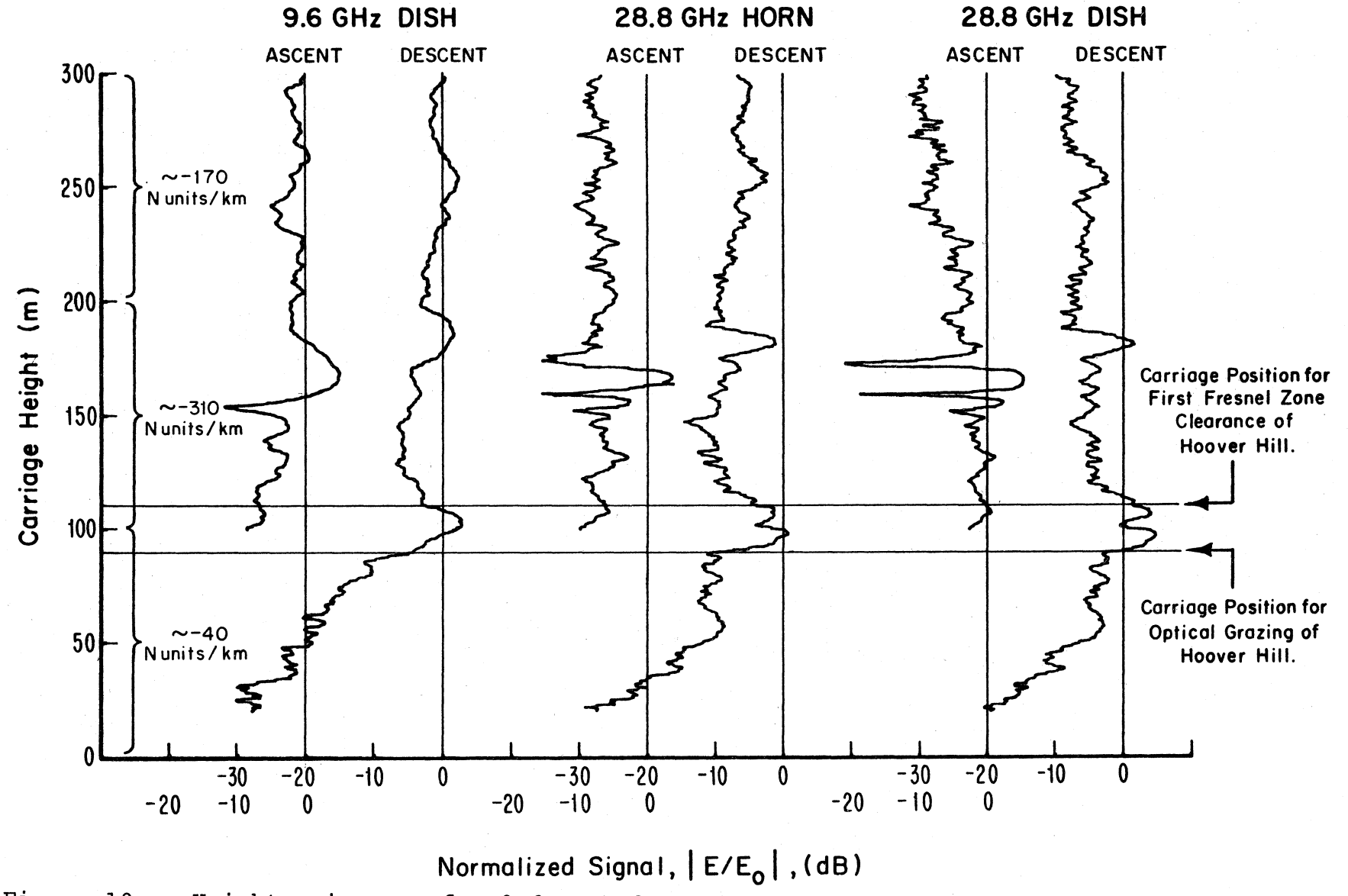

Figure 10. Height-gain runs for 9.6 GHz, 28.8 GHz horn and 28.8 GHz dish on July 26, 1979. 1 sample/sec. σ^2(9.6 GHz) ≃ 11.47 dB^2 , σ^2(28.8 GHz horn) ≃ 7.26 dB^2 , σ^2(28.8 GHz dish) ≃ 17.696 dB^2. Starting time for ascent was 0722:00.

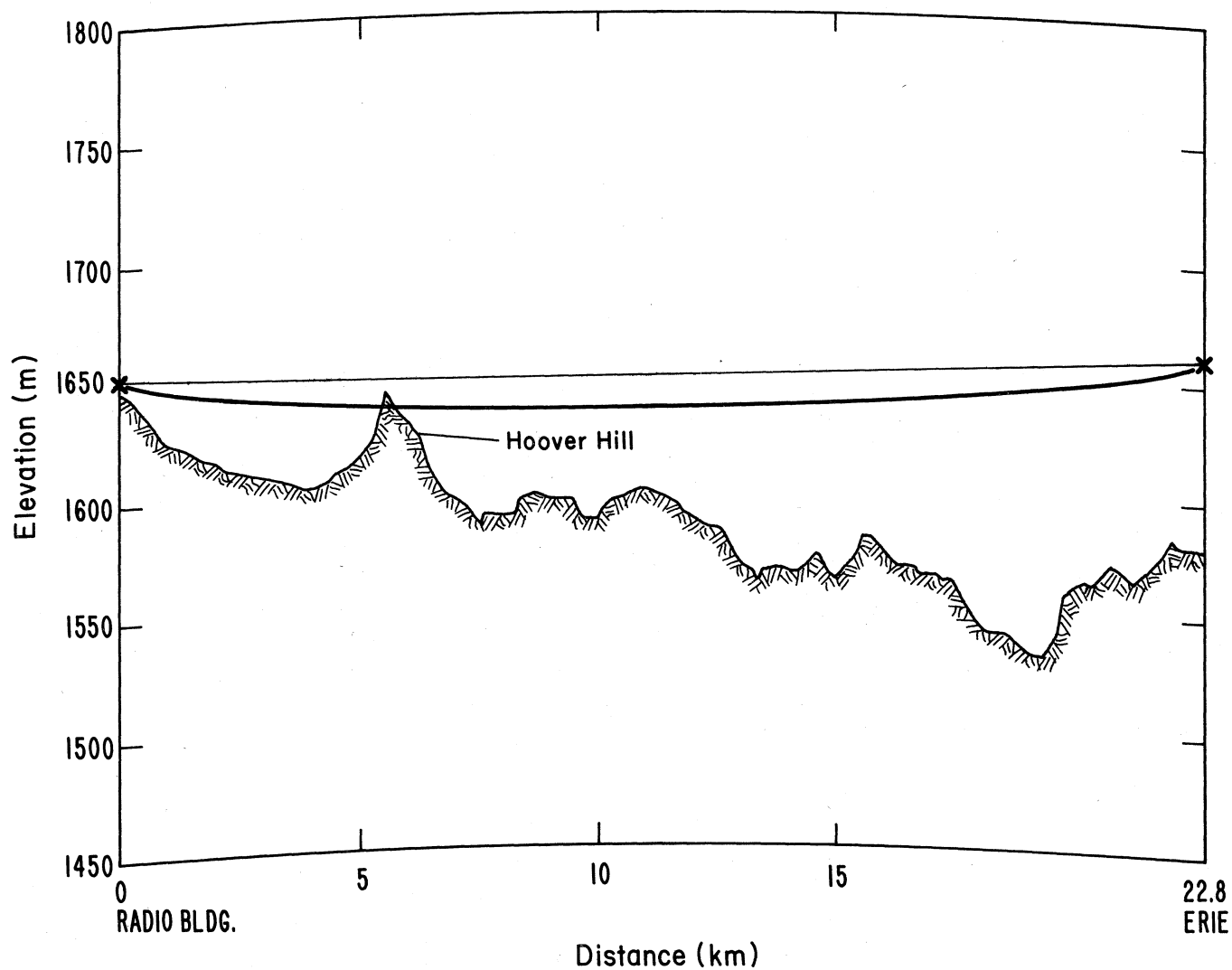

Figure 11. First Fresnel zone for transmitter at 80 m above the ground at the BAO tower. Profile drawn using 4/3 earths effective radius.

transmitter at 80 m and the path profile drawn using a 4/3 effective earths radius. The 28.8 GHz dish signal in the height range 80-110 m appears somewhat too high above the free-space value. However, several calibration checks failed to uncover any discrepancy. The fades and enhancements at a height of about 170 m on ascent are the result of the "extreme ducting" conditions that existed causing the fields to enhance and fade on either side of this deep radio hole. Signal variations with height of nearly 30 dB are observed in this height region. The 28.8 GHz signal went through 3 cycles of lobing while the 9.6 GHz signal went through 1 cycle during the ascent through the 170 m height. The location of this interference phenomena on descent seemed to occur at about 180 m indicating some upward shift in the layer height as a function of time. The layer only has to move about 24 m to produce a half-wavelength change in a multipath ray reflected at midpath at 28.8 GHz. We claim the results in Figure 10 correspond to the existence of a radio hole. On either side of the radio hole the field will enhance corresponding to the wave diffracting energy around the edges of the hole into the hole. In the hole itself the field is quite small. These features fit the observations in the region where the duct exists (i.e. 100-200m in Figure 10). Also, the field will fall and rise at rates which increase with frequency and this effect is observed in Figure 10 as well. In the radio hole the density of rays goes to zero.

In Figure 12, we show height-gain runs for the 9.6, 28.8 GHz horn and 28.8 GHz dish signals at 1407 MDT on July 26, 1979. During this time period when the atmosphere has returned to a well-mixed condition, the signal strength has 5 dB variations caused by scattering from the turbulent eddies and large fades or enhancements were not present. Figure 12 also shows the absence of multipath caused by possible ground reflections and adds support to our claim of no ground multipath.

Figures 13a and 13b show spatial correlation of the 28.8 GHz horn and 28.8 GHz dish and 28.8 GHz dish and 9.6 GHz dish respectively. These Figures correspond to the height-gain runs in Figure 10. In Figure 13a, the 28.8 GHz horn and dish correlation is offset about 1 lag (3 m) horizontally. The offset in the maximum correlation from zero lag in Figure 13a may correspond to a cross wind moving the refractivity structure horizontally. The spatial correlation in

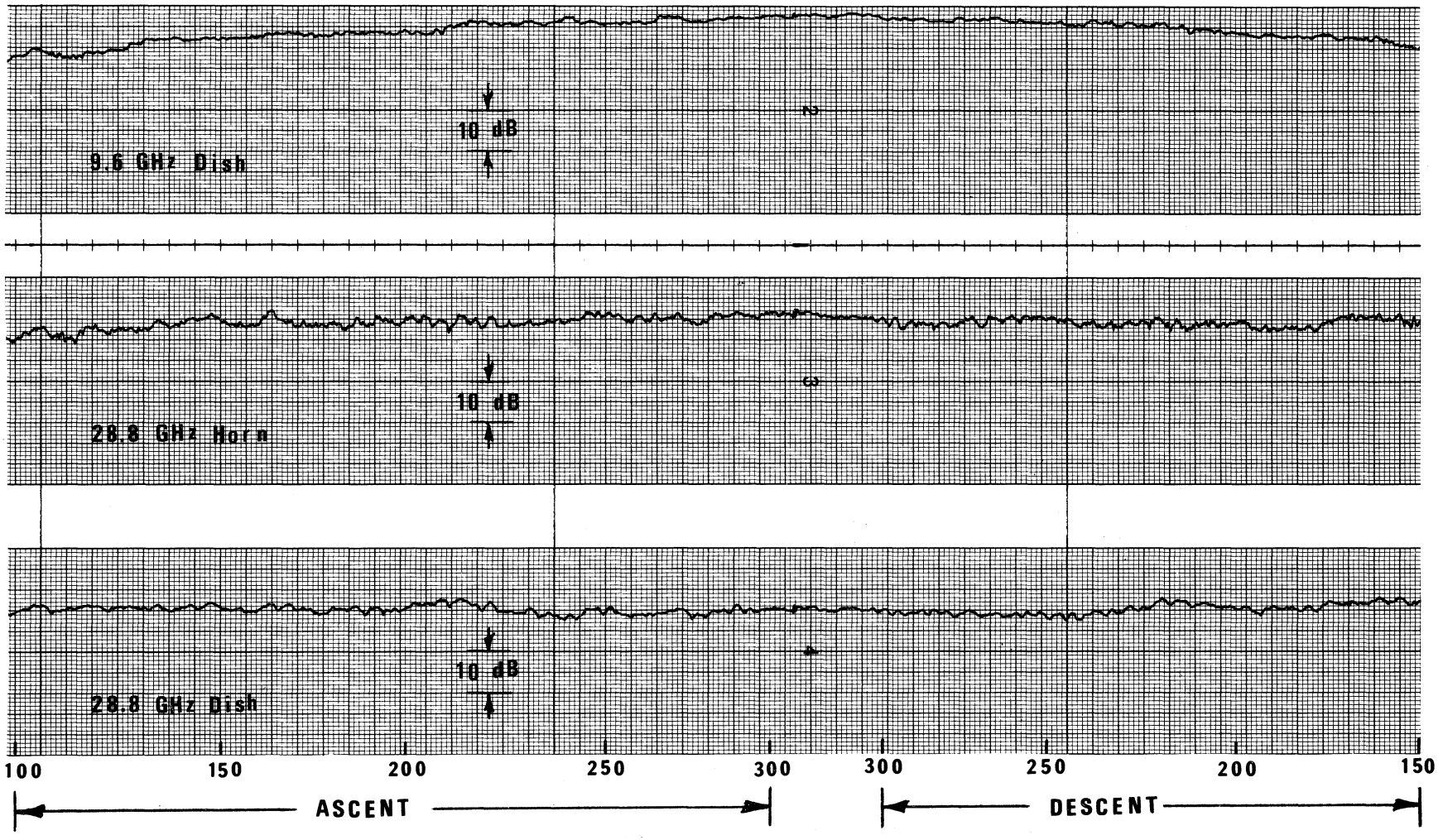

Figure 12. Height-gain runs for 9.6, 28.8 GHz horn and 28.8 GHz dish signals at 1407 MDT, July 26, 1979.

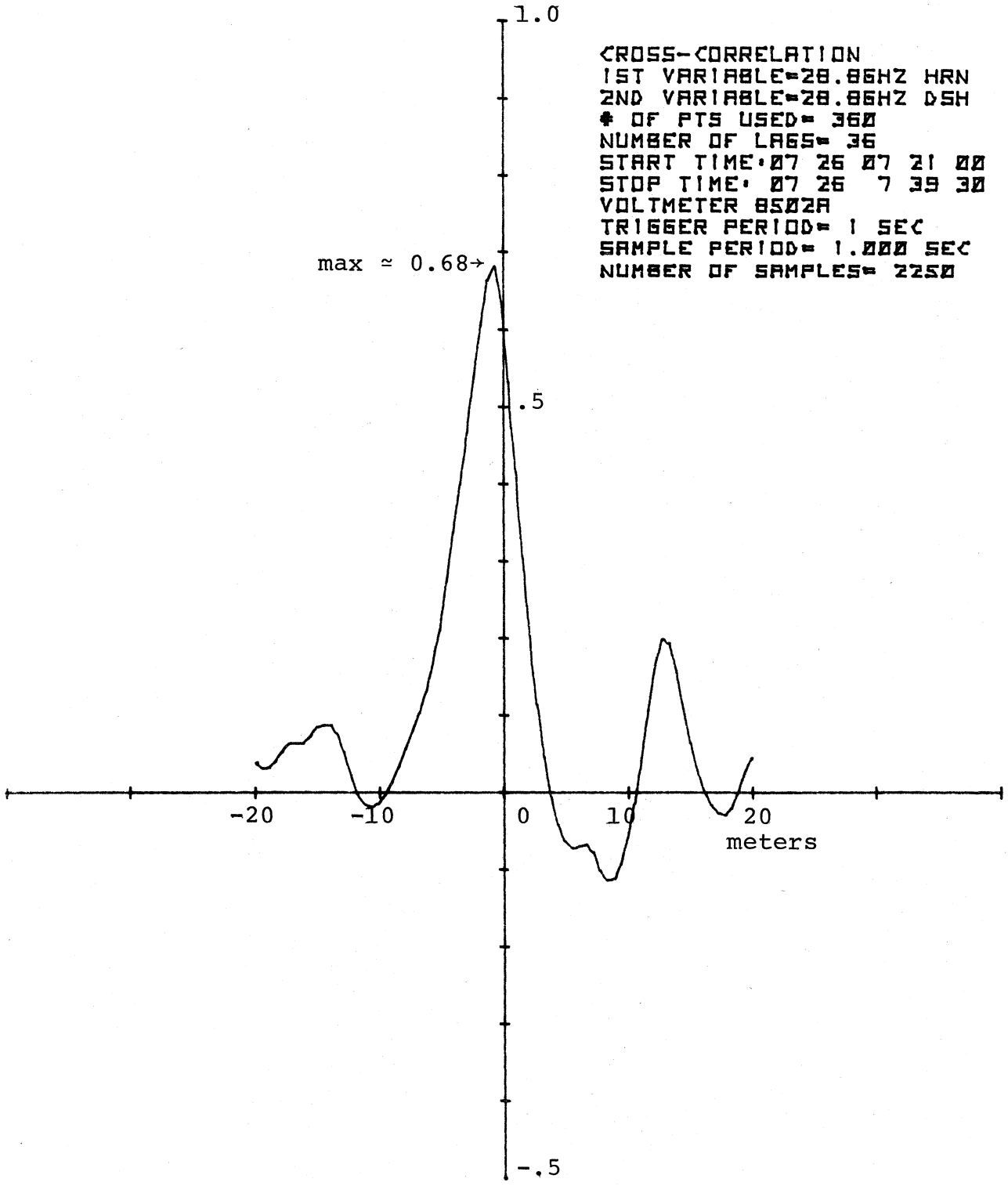

Figure 13a. Spatial correlation of 28.8 GHz horn and 28.8 GHz dish signals from 0722:00 to 0727:59 on 7/26/79.

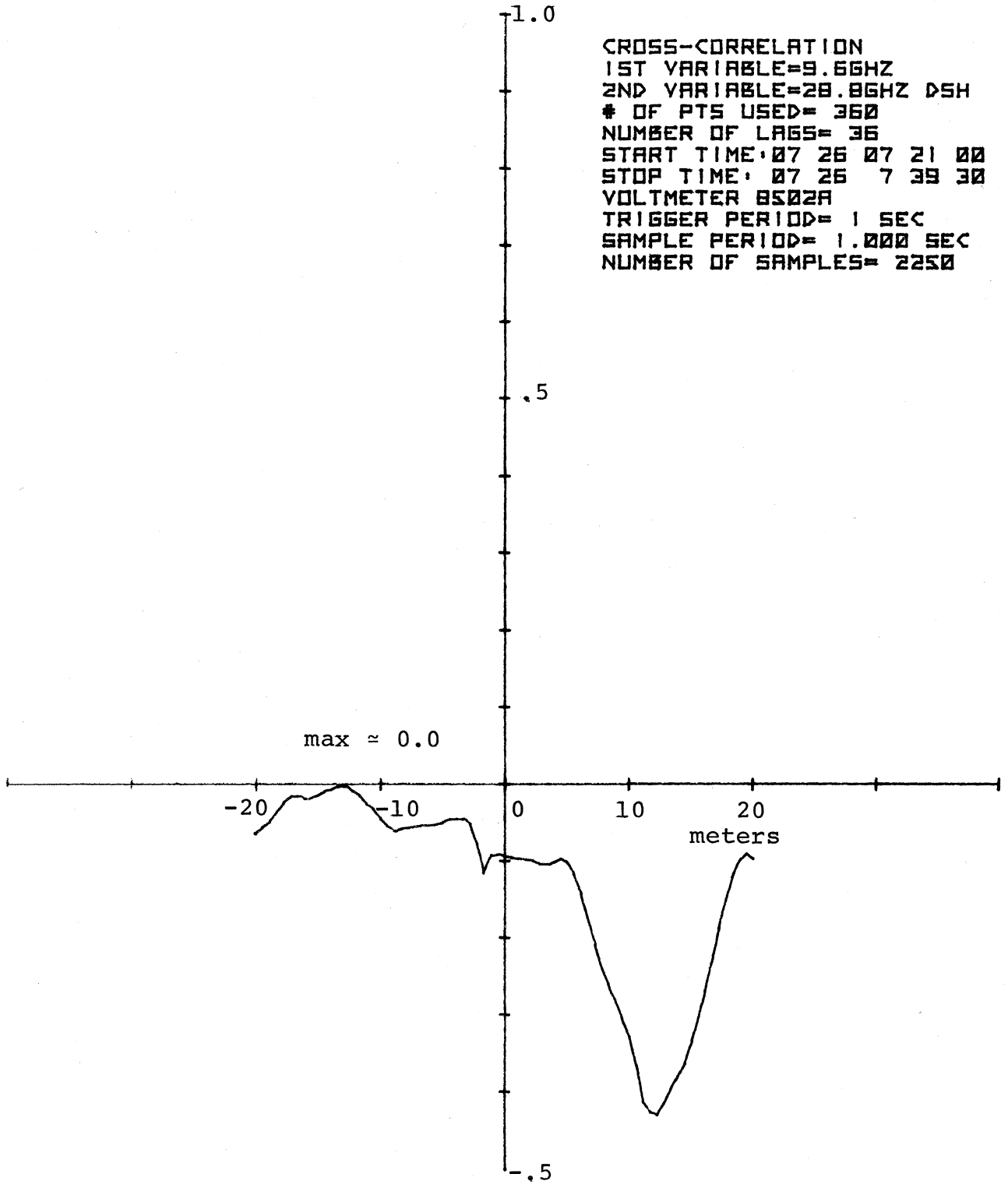

Figure 13b. Spatial correlation of 28.8 GHz dish and 9.6 GHz horn signals from 0722:00 to 0727:59 on 7/26/79.

Figure 13a gives some insight into antenna separation to be used in space diversity. The spatial distance in Figure 13a from peak correlation to minimum correlation is about 10 m. This would be an optimum separation for vertical space diversity for this particular data set.

Figure 14 shows the height-gain runs for ascent and descent starting at 0802:22 and ending at 0817:18 on 7/26/79. The 0 dB point corresponds to the free-space signal strength. For carriage heights greater than the height corresponding to the first Fresnel zone clearance of Hoover Hill (i.e., 110 m) the greatest signal variations occurred in the height range 160 to 210 m. In this height-gain region the 9.6 GHz and 28.8 GHz signals faded and enhanced at the same heights indicating the duct was "cut-off" for the dominant mode at 9.6 GHz but supported the higher-order mode in Figure 14 having two full cycles of lobing. The gradient of refractive index in the duct in Figure 10 was about -310 N-unit/km while the gradient in the duct in Figure 14 was about -320 N-unit/km. Figures 15a and 15b show the spatial correlation for the height-gain run in Figure 14.

Figure 16 shows the height-gain runs for ascent and descent starting at 0830:10 and ending at 0850:46 on July 26, 1979. The 0 dB point corresponds to the free-space signal strength. In the height range from about 115 m to 160 m on ascent, the 9.6 GHz signal went through one-half cycle variation while the 28.8 GHz signal went through about 3 half-cycle variations indicating the duct width increased from its value for the height-gain run in Figure 14. The conjecture is that from 0800 in Figure 14 to 0830 in Figure 16 the characteristics of the duct changed sufficiently to cause the 9.6 GHz signal to go through one cycle of variation in the height range 115 to 160 m in Figure 16 as opposed to two cycles in Figure 14. This also could have been caused by the duct width changing. Figures 17a and 17b show the spatial correlations for the same time period as Figure 16.

Figure 18 shows the height-gain runs for ascent and descent starting at 0855:20 and ending at 0912:51 MST on July 26, 1979. The 0 dB point corresponds to the free-space signal strength. In the height range from about 140 m to 170 m on ascent, the 9.6 GHz signal went through one-half cycle variation while the 28.8 GHz signal went through three half-cycles of variation. This would imply that the

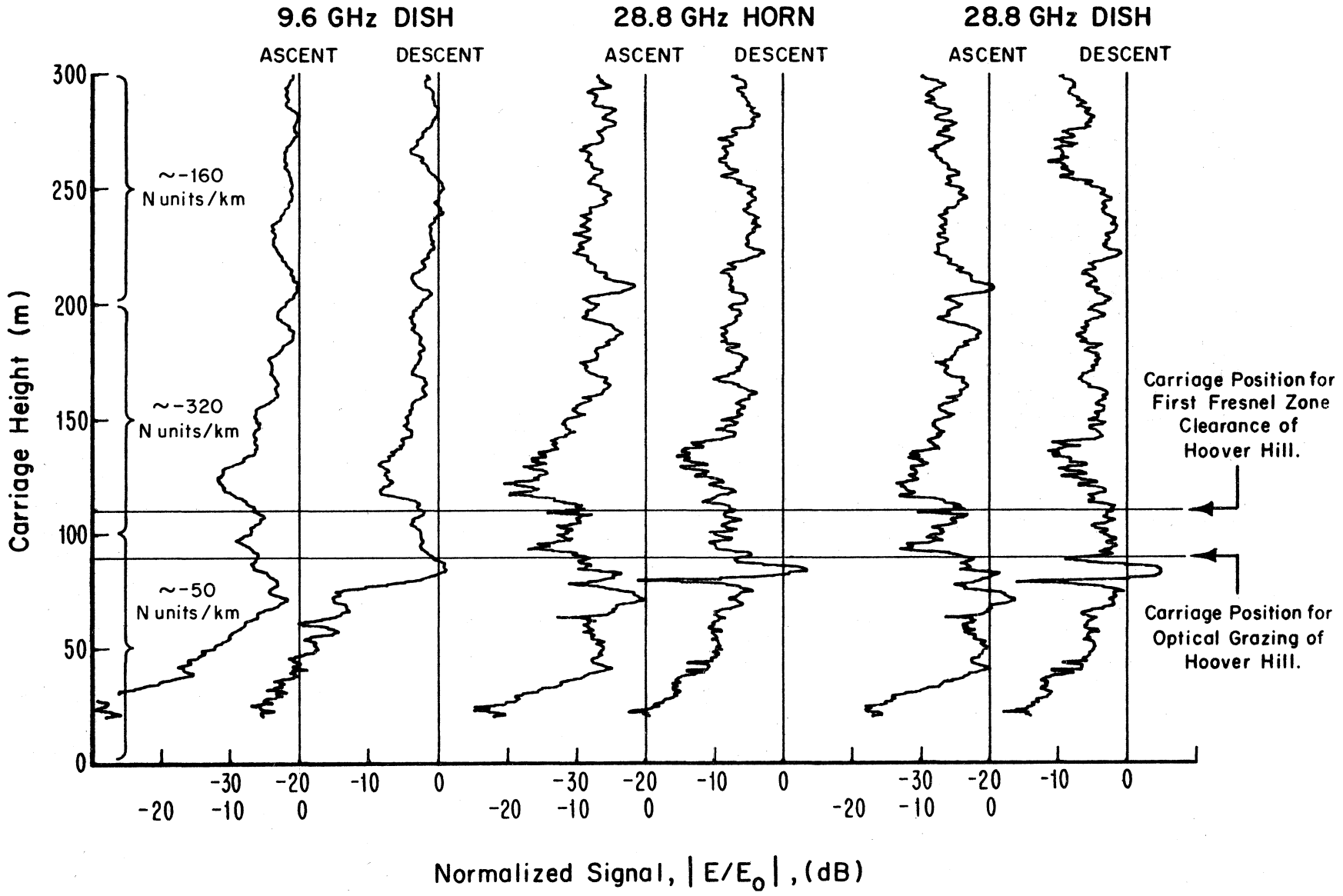

Figure 14. Height-gain runs starting at 0800 and ending at 0817 on 7/26/79. 1 sample/sec. σ^2(9.6 GHz)≃8.43 dB^2, σ^2(28.8 GHz horn)≃12.07 dB^2, σ^2(28.8 GHz dish)≃6.38 dB^2.

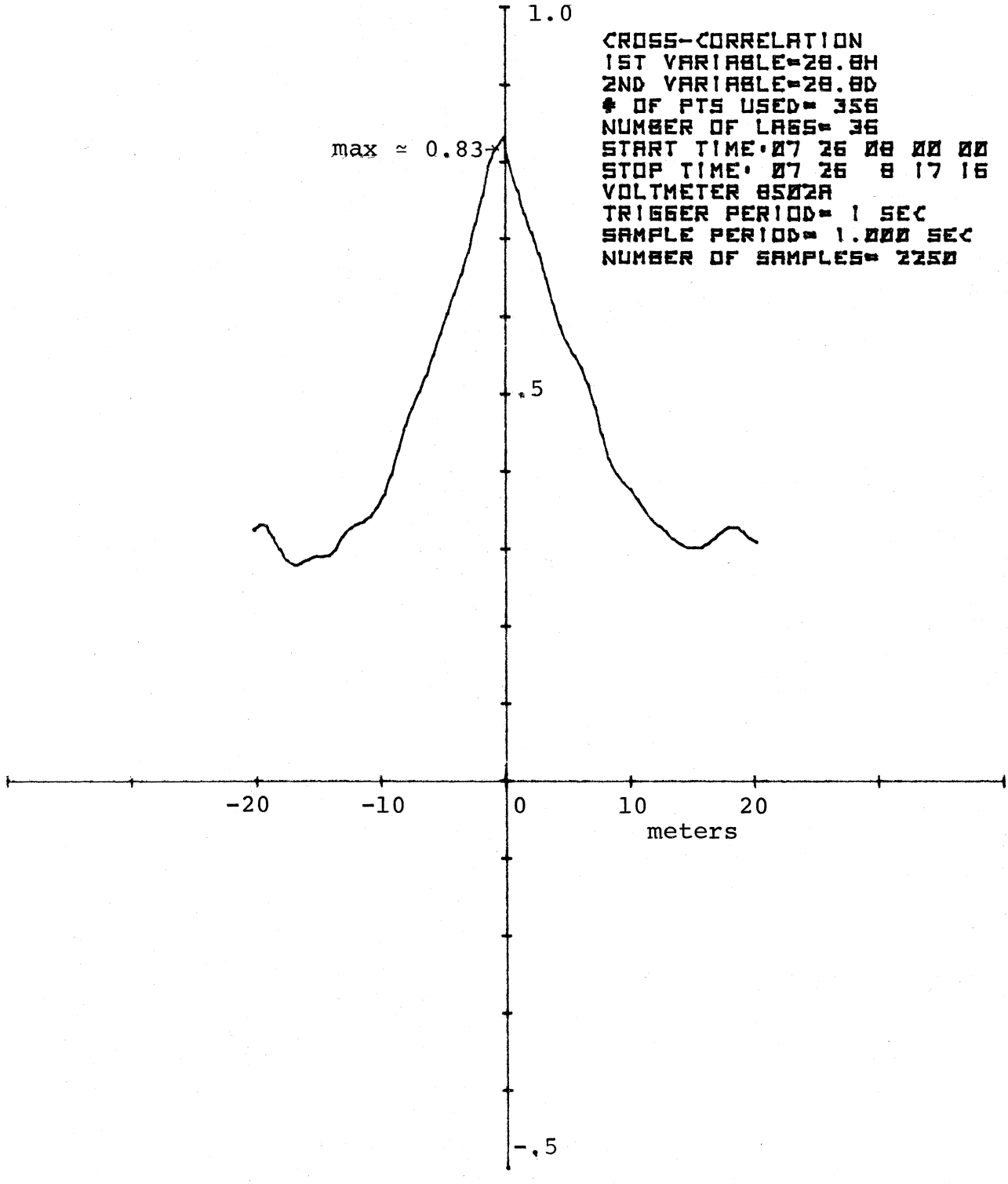

Figure 15a. Spatial correlation of 28.8 GHz horn versus 28.8 GHz dish for 0802:22 to 0808:16 on 7/26/79.

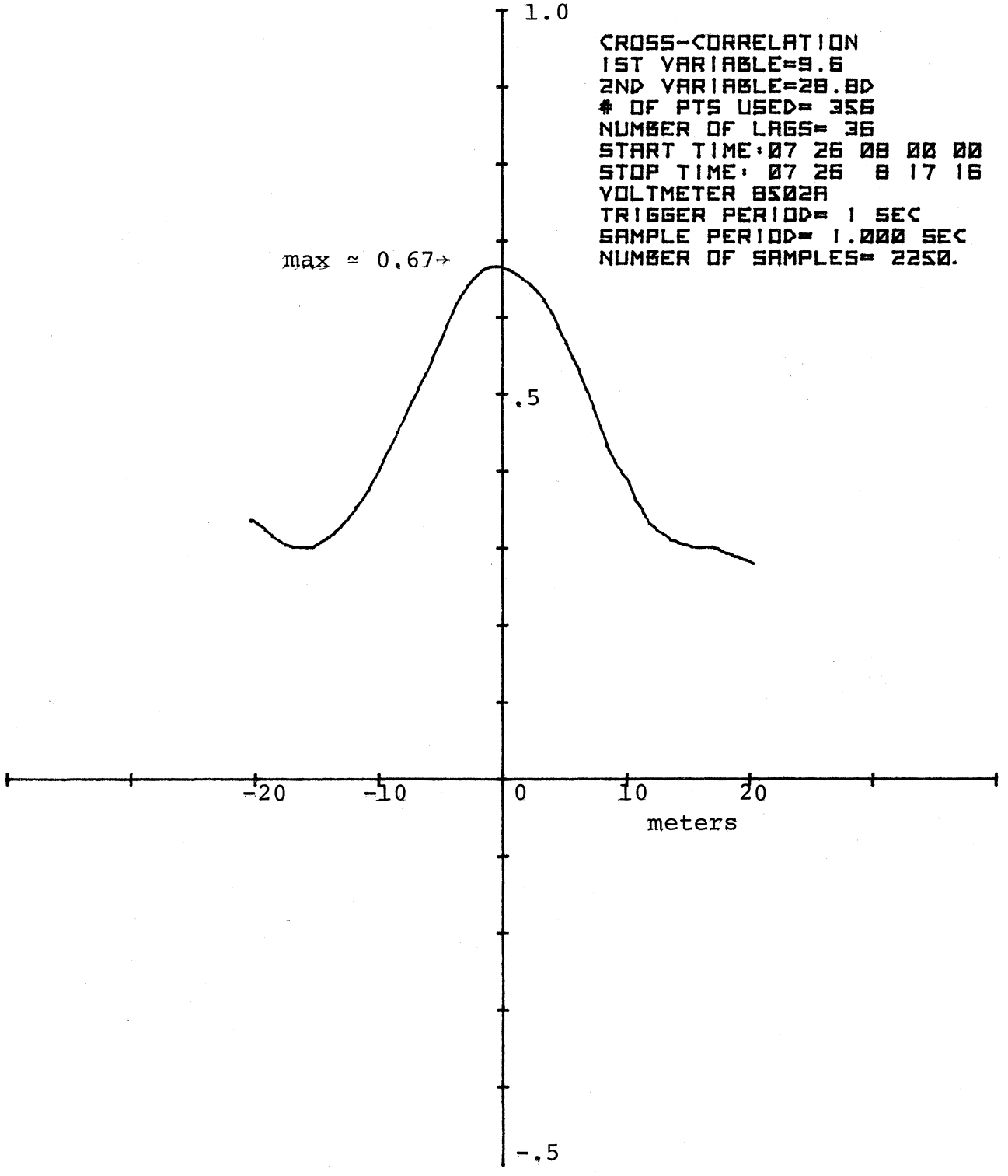

Figure 15b. Spatial correlation of 9.6 GHz dish versus 28.8 GHz dish from 0802:22 to 0808:16 on 7/26/79.

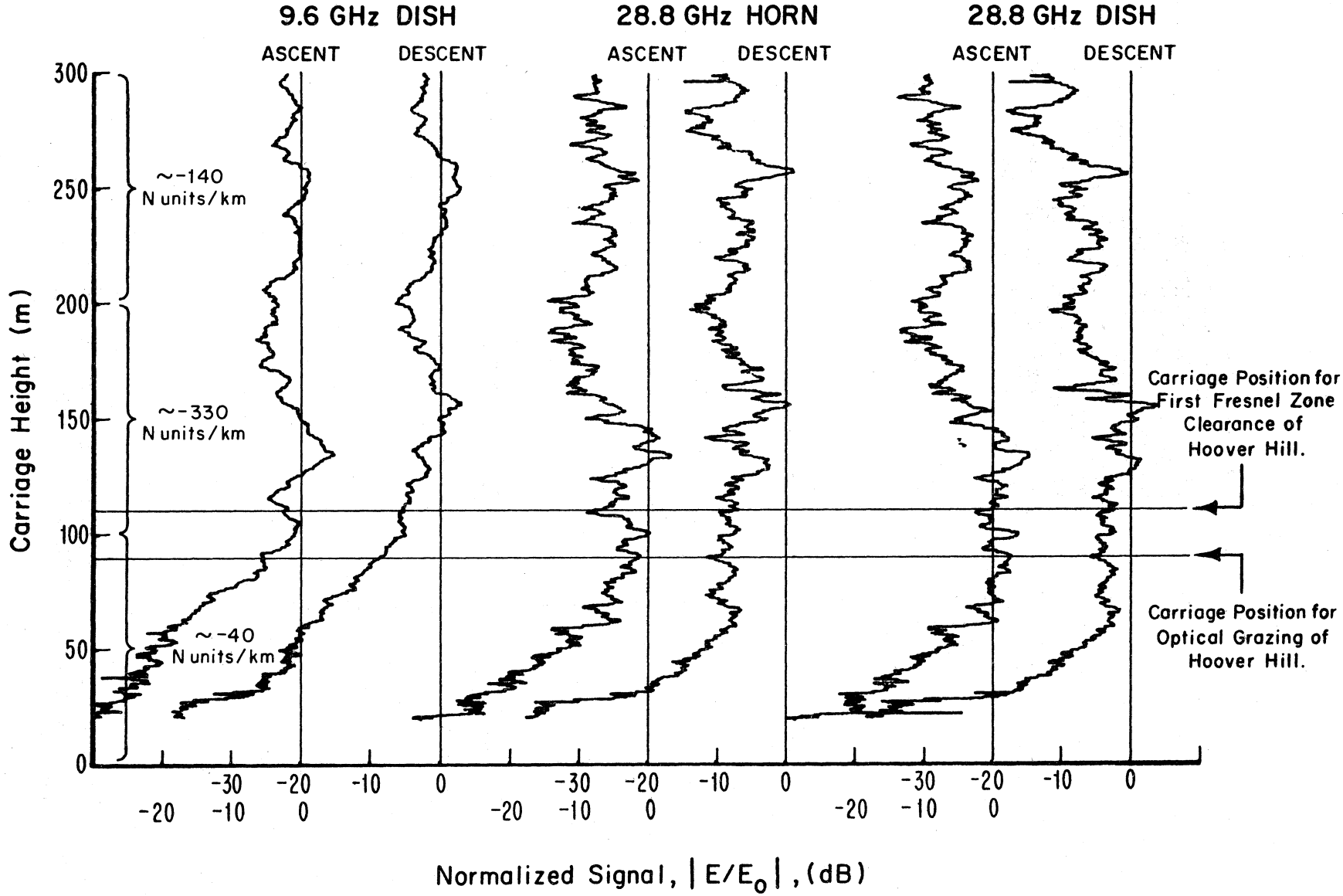

Figure 16. Height-gain runs for 9.6 GHz, 28.8 GHz horn and 28.8 GHz dish from 0830:10 to 0850:46 on 7/26/79. 1 sec. samples. σ^2(9.6 GHz) ≃ 5.58 dB^2, σ^2(28.8 GHz horn) ≃ 13.00 dB^2, σ^2(28.8 GHz dish) ≃ 17.92 dB^2.

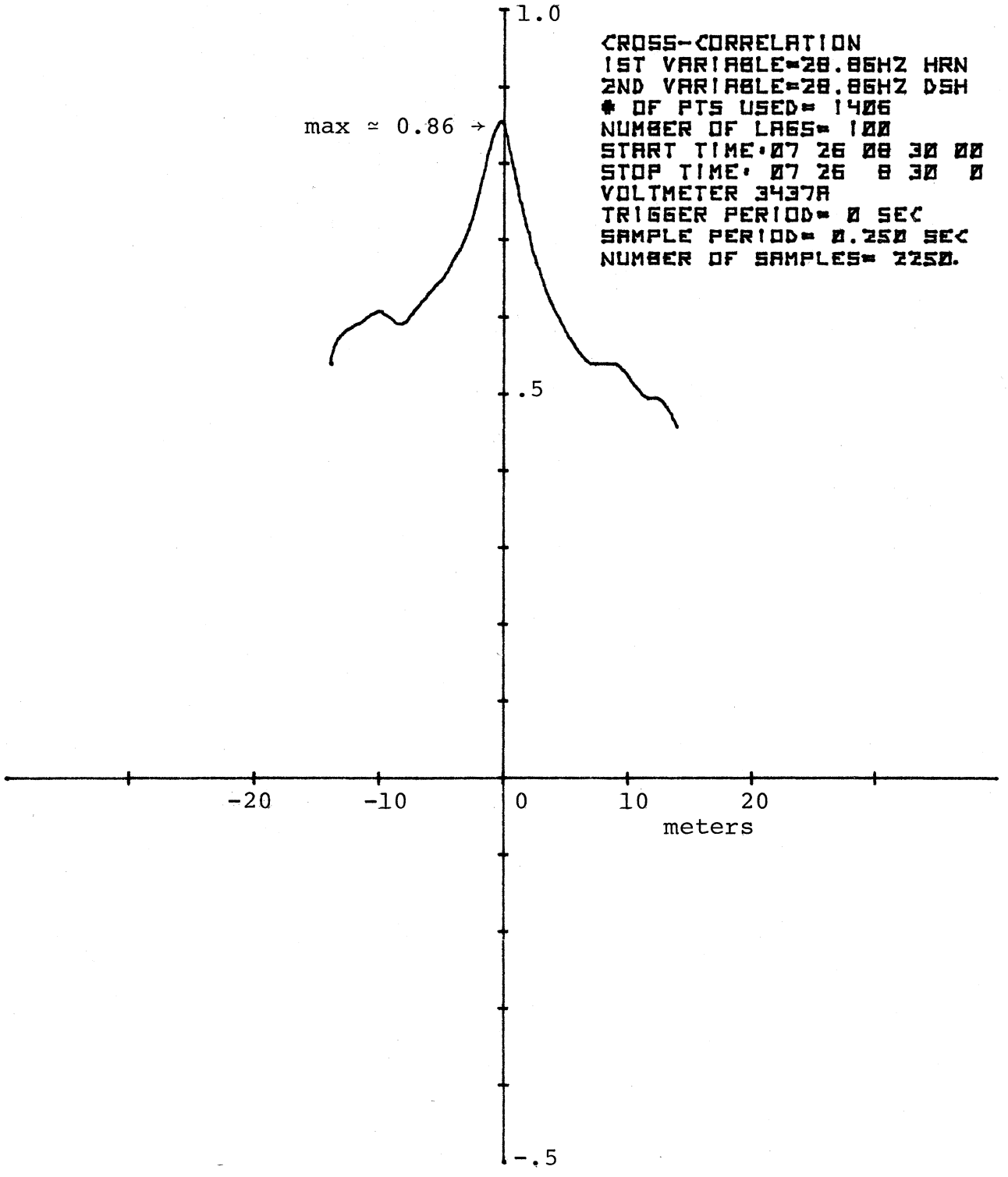

Figure 17a. Spatial correlation for 28.8 GHz horn versus 28.8 GHz dish from 0832:25 to 0838:16 on 7/26/79.

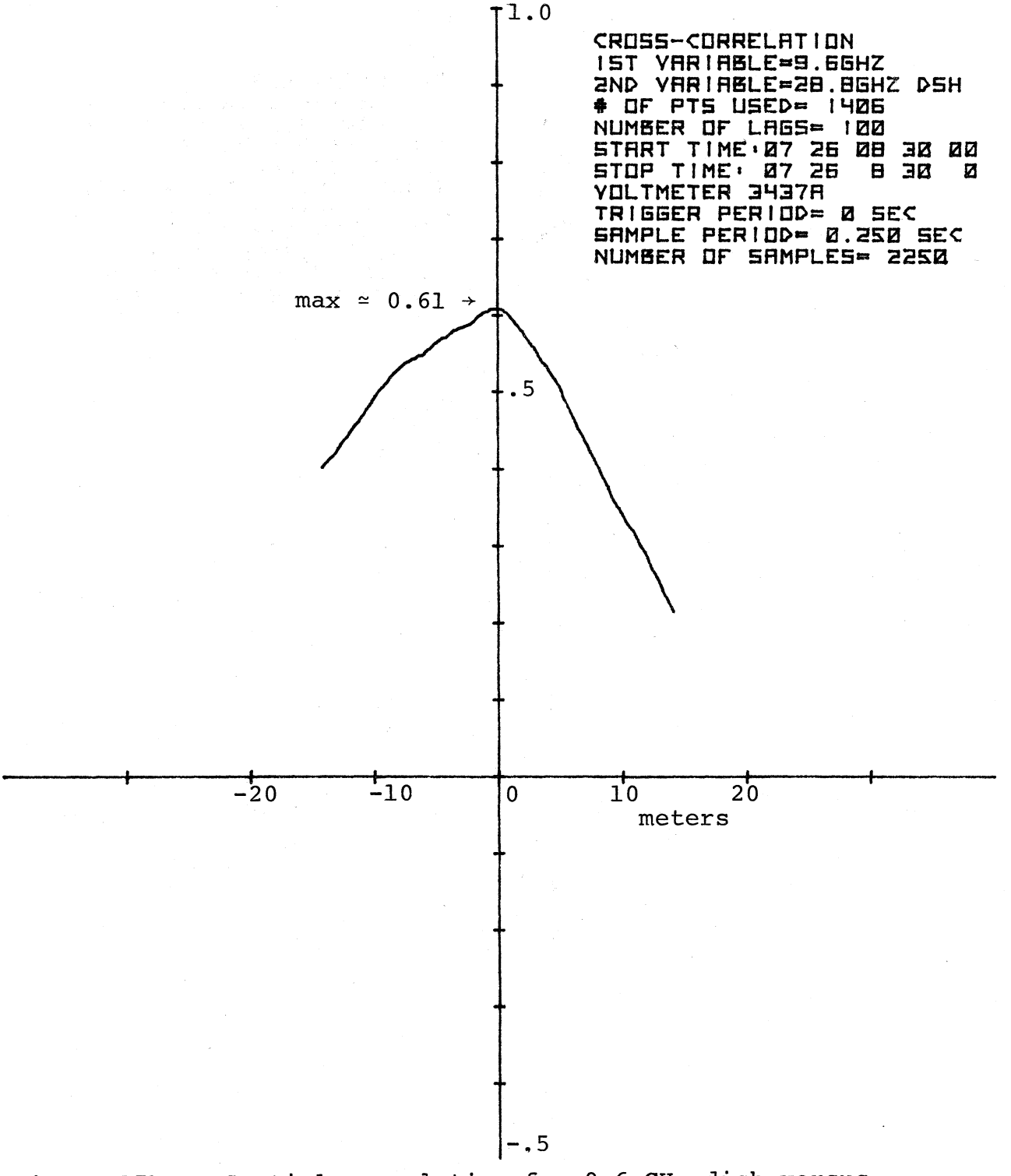

Figure 17b. Spatial correlation for 9.6 GHz dish versus 28.8 GHz dish from 0832:25 to 0838:16 on 7/26/79.

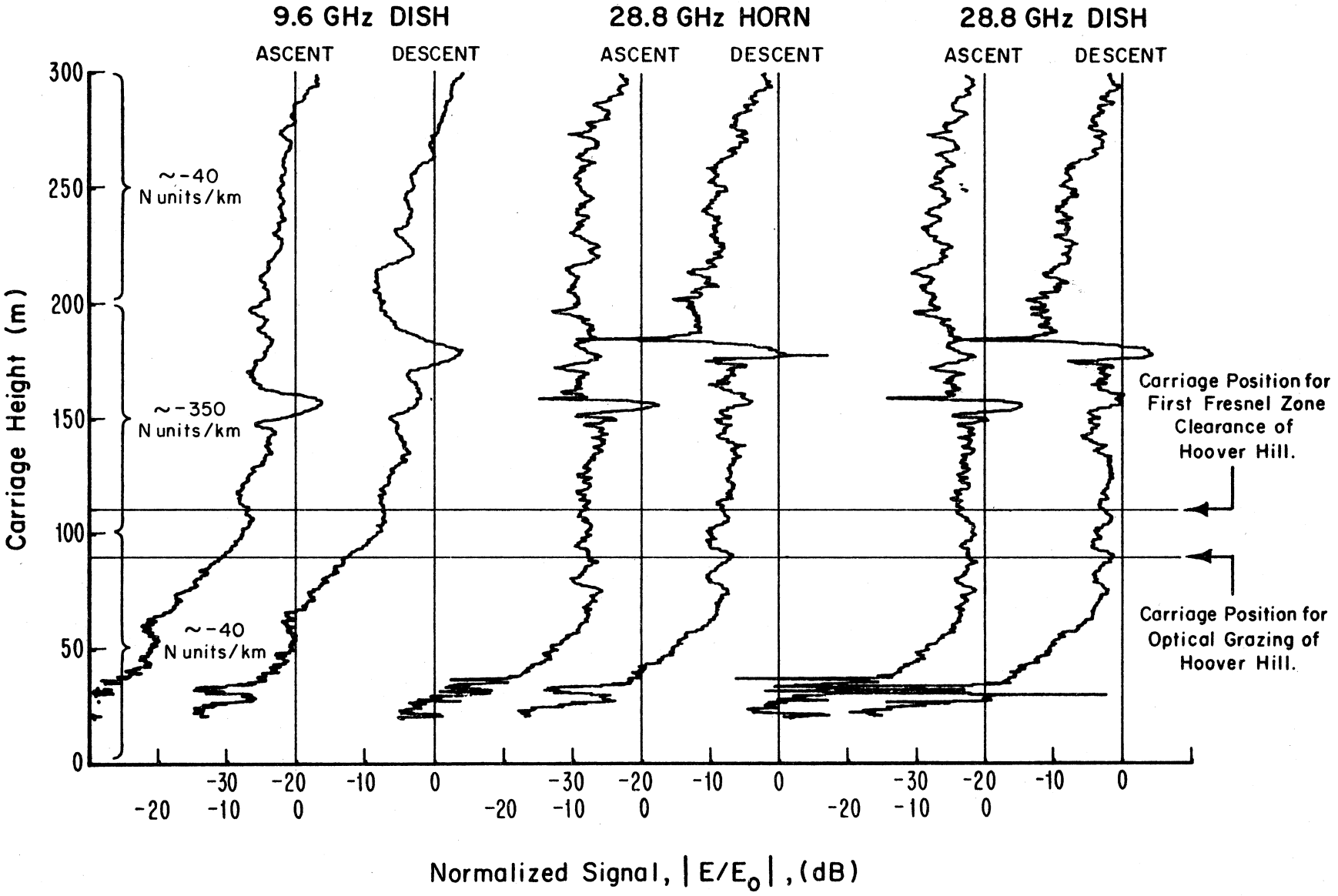

Figure 18. Height-gain runs starting at 0855:20 and ending at 0912:51 on 7/26/79. 1 sample/sec. σ^2(9.6 GHz) ≃ 8.93 dB^2 , σ^2(28.8 GHz horn) ≃ 6.13 dB^2 , σ^2(28.8 GHz dish) ≃ 6.94 dB^2.

duct geometry for this time period was comparable with that for the height-gain run in Figures 17 and 10.

Figures 19a and 19b show the correlations for the time period 0857:22 to 0903:16 on July 26, 1979.

6. CONCLUSIONS

Examples are shown of multipath fading for both fixed transmitter/receiver locations and height-gain runs observed on a 23 km path from the BAO tower in Erie, Colorado, to the Radio Building in Boulder, Colorado. By comparing the received signal during time periods when the atmosphere was in a normal condition with those periods when the atmospheric structure produced a duct, we conjecture that the fading was the result of atmospheric multipath and not ground reflections. In particular, we believe we observed some examples of "radio holes".

We believe these preliminary results are interesting from the standpoint that the extremely short delays between the 1st and 2nd components in a 3-ray model for atmospheric multipath may be resolvable using the BAO tower at Erie and should contribute toward a better understanding of the 3-ray model.

There is more research that must be performed before the possibility of ground reflections can be discounted. This research should take the form of 1) recording the refractivity structure with a finer spatial resolution than the 50 m increments used in obtaining the results in this report, 2) use Hufford's full wave solution for the received signal as a function of height and make comparison with the observed height-gain runs, 3) use Rummler's model for estimating the parameters in a 3-ray model for the transfer function.

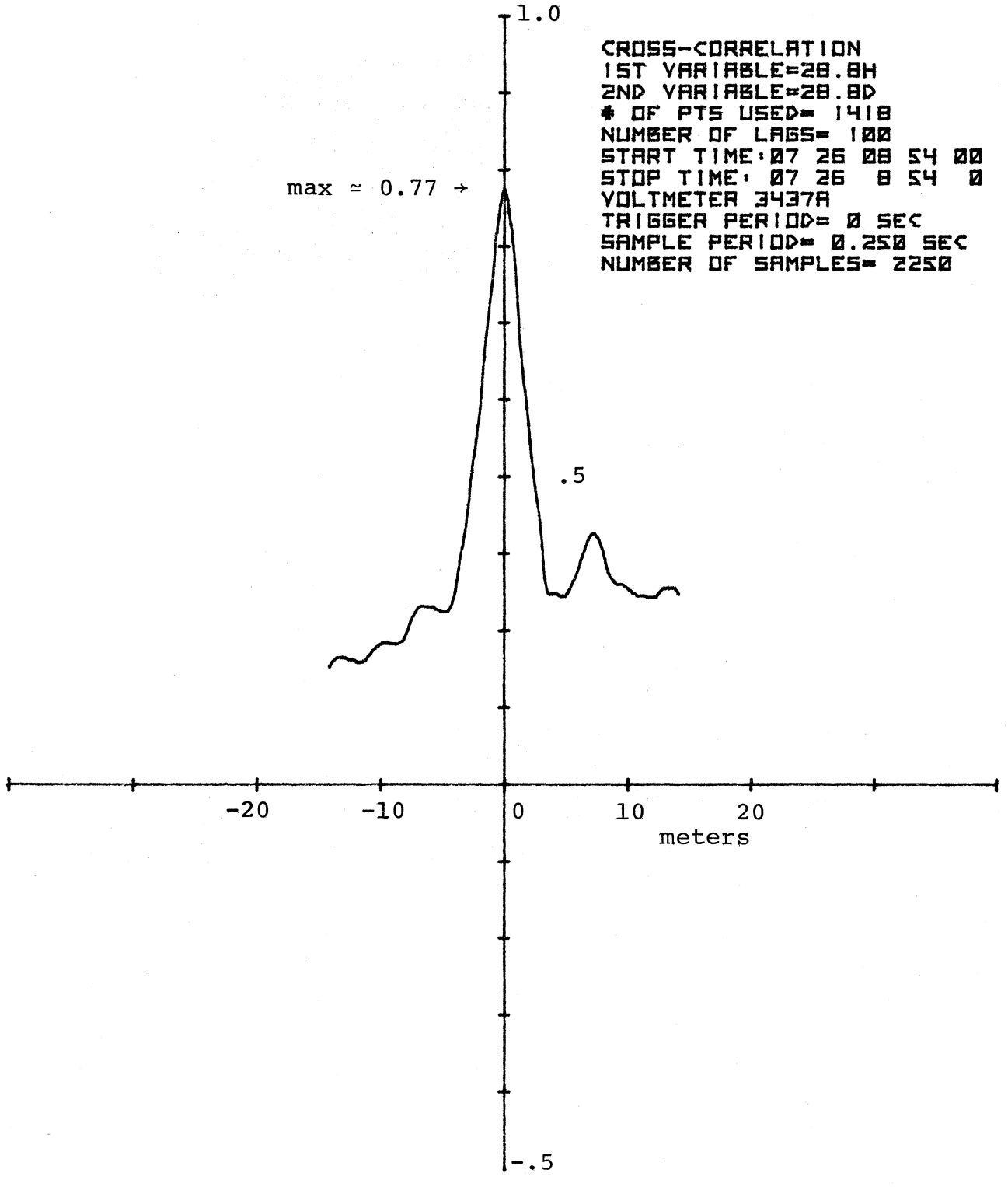

Figure 19a. Spatial correlation of 28.8 GHz horn with 28.8 GHz dish for 0857:22 to 0903:16 on 7/26/79.

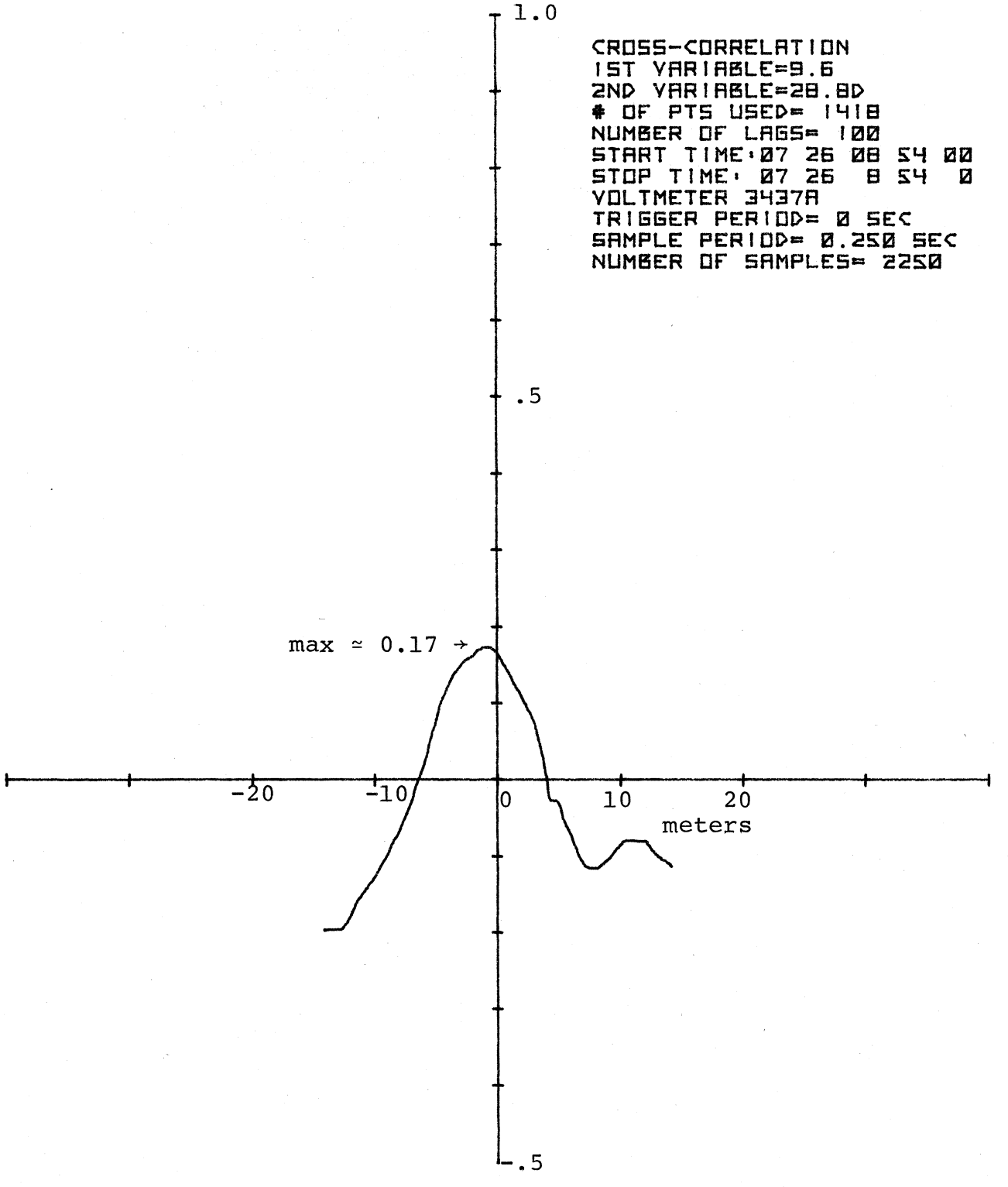

Figure 19b. Spatial correlation of 9.6 GHz dish with 28.8 GHz dish for 0857:22 to 0903:16 on 7/26/79.

7. BIBLIOGRAPHY

1) Ament, W. S., W. Binnian, W. W. Carter, M. Katzin, and D. T. Olmsted (1962), Microwave propagation measurements over the Pacific Ocean, 1946, NRL Report 5687, U. S. Naval Research Lab., Washington, D. C.

Extended range observations along paths in Okinawa and the Philippines.

2) Anderson, C., S. Barber, and R. Patel (1977), Propagation experiments show path to excess, Telesis, Dec., Special issue: DRS-B digital radio system, 180-185.

Anderson et al. made 8 GHz measurements of a digitally modulated signal over paths 45-50 km. The inband distortion was studied in the frequency domain by measuring the amplitude and delay at five frequencies across a $\pm$ 15 MHz band during multipath fading. The effects of frequency and space diversity were also studied.

3) Babler, G. M. (1972), A study of frequency selective fading for a microwave line-of-sight narrowband radio channel, BSTJ, Vol. 51, No. 3, March, 731-757.

The temporal and spectral characteristics of a 6 GHz signal subject to multipath were estimated using a field of 62 coherent tones spaced 550 kHz apart and centered on 70.4 MHz. The transmitter translated the 33.55 MHz wide tone to a 6.0342 GHz carrier and propagated along the 26 mile Palmetto-Atlanta, Georgia path. Two antennas were used to receive the signal; a horn reflector antenna having a 1.25° half-power beamwidth and a 6 ft. dish having a 2° half-power beamwidth. The conclusion regarding beamwidth is "the selective fading structure as observed in a narrow-band radio channel at these frequencies is insensitive to the beamwidth or to the precise vertical location of the antenna." The statistical behavior of the envelope of a fading signal follows the fade depth distribution

$$P(V \leq L) \alpha\ L^2$$

where the fade depth = -20 Log L, and V is the amplitude of the received signal.

4) Barnett, W. T. (1972), Multipath propagation at 4, 6 and 11 GHz, BSTJ, Vol. 51, No. 2, Feb., 321-361

The empirical estimate for the "total time faded",

$$P = rL^2$$

where L is the normalized algebraic value of the envelope voltage (fade depth in dB = $-20\ \mathrm{Log}_{10} L$) and

$$r = c\left(\frac{f}{4}\right) D^3 \times 10^{-5}$$

where

$$c = \begin{cases} 1, & \text{average terrain} \\ 4, & \text{over-water and Gulf Coast} \\ 1/4, & \text{mountains and dry climate} \end{cases}$$

f is the frequency and D is the path length.

5) Bean, B. R. (1959), Climatology of ground-based radio ducts, NBS 63D, 29-34.

Bean analyzed rawinsonde data from 3 regions in the U.S. and observed ground-based ducts in many profiles, with a maximum lapse rate of -420 N-units/km and an average thickness of about 100 m.

6) Bean, B. R., and B. A. Cahoon (1959), Effect of atmospheric horizontal inhomogeneity upon ray tracing, J. Res. NBS, 63D, 287-292.

Bean and Cahoon report abrupt horizontal changes in refractive index associated with land-sea breezes, and special events such as storms and frontal passages.

7) Chang, H. T. (1971), The effect of tropospheric layer structure on long-range VHF radio propagation, IEEE Trans. Ant. Prop. AP-19, 751-756.

Explained propagation within a duct in terms of mode theory.

8) Clemow, D. B., and E. H. Bruce-Clayton (1963), Long-range VHF air/ground communications, Radio and Electron. Engr. 25, 17-30.

Clemow and Bruce-Clayton studied enhanced field strength and extended range in the area of the Persian Gulf.

9) Cowan, L. W. (1953), A radio climatology survey of the U.S., Proc. Conf. on Radio Meteorol., Univ. of Texas, Austin, Texas.

Cowan noted that ducting gradients are found in as many as 40% of radiosonde observations during some months, and that most occur within the first km above the earth's surface.

10) Crain, C. M. (1953), Refractometer measured tropospheric index-of-refraction profiles, Vols. I and II, Univ. of Texas, EERL Rept. 6-02.

Using an airborne microwave refractometer, Crain measured refractive index profiles off the coast at San Francisco to distances of 150 mi at elevations up to 12,000 ft. He describes the west coast as characterized by a marine layer immediately above the sea surface, with a warm dry layer above it. This produces a strong inversion, with a superrefractive layer, which may range in elevation from a few hundred feet to 5000 ft.

11) Crawford, A. B., and W. C. Jakes, Jr. (1952), Selective Fading of Microwaves, BSTJ, Vol. 31, No. 1, Jan., 68-90.

Angle-of-arrival measurements at 1.25 cm and frequency selective fading measurements over a 450 MHz band on a 22.8 mile path from Murray Hill, N. J. to Holmdel, Lab, N.J.

12) Davies, M. C. (1976), The effect of multipath propagation on the performance of 4-level phase-shift-keyed digital microwave radio-relay systems, Post Office Telecommunications, Research Dept. Report No. 562, Oct., The Post Office Research Centre, Martlesham, Heath, Ipswich, U.K.

The effect of 3 ray multipath distortion on 4 QPSK digital systems in the presence of wide-band Gaussian noise is calculated by computer simulation.

13) DeLange, O. E. (1952), Propagation studies at microwave frequencies by means of very short pulses, BSTJ, Vol. 31, No. 1, Jan., 91-103.

One of the first short pulse experiments for investigating multipath. Microwave pulses with a duration of 3 ns were transmitted over a 22 mile path from Murray Hill, N.J. to Holmdel, N.J. The carrier frequency was 4 GHz. Multipath delays of 7 ns were observed. Minimum resolution was 0.7 ns.

14) Dougherty, H. T., and W. J. Hartman (1977), Performance of a 400 Mbit/s systems over a line-of-sight path, IEEE Trans. on Communications, Vol. Com-25, No. 4, April, 427-432.

The authors detected atmospheric multipath by examining the notch in the received spectrum as a multipath component moving through the path geometry. An example of the fading in a "rapidly-changing" atmosphere is shown in Figure B-1.

15) Edinger, J. G. (1959), Changes in the depth of the marine layer over the Los Angeles basin, J. Meteorol. 16, 219-226.

Edinger reported rapid changes in the marine layer with time of day, season, and large-scale weather changes.

16) Flock, W. L., R. C. MacKey, and W. D. Hershberger (1960), Propagation at 36,000 Mc in the Los Angeles basin, IRE Trans. AP-8, 235-241.

Flock et al. noted that the marine layer is about 1500 ft. thick near Los Angeles, but there is a considerable variation from near zero to about 4000 ft.

17) Guinard, N. W., J. Ransome, D. Randall, C. Purves, and P. Watkins (1964), Propagation through an elevated duct. Tradewinds III, IRE Trans. AP-12, 479-490.

Guinard et al. observed the greatly extended ranges that may result from strong, persistent atmospheric layers on airline routes from San Diego to Hawaii.

18) Hartman, W. J., and D. Smith (1975), Tilting antennas to reduce line-of-sight microwave link fading, Final report prepared for U. S. Dept. of Transportation, report no. FAA-RD-75-38, Federal Aviation Administration, Systems Research and Development Service, Washington, D. C. 20590.

Figure B2 shows a time series for a 8.1 GHz signal over a 50 km path between Fowler and Boone, Colorado. The authors found that ground reflections could be eliminated by proper antenna tilting.

19) Katzin, M. (1957), On the mechanisms of radar sea clutter, Proc. IRE 45, 44-54.

Propagation studies over the Atlantic Ocean.

20) Kerr, D. C. (1951), Propagation of short radio waves, Dover, N. Y.

Pages 140-174 give a detailed description of calculating the characteristic eigenvalues and eigen functions in a bilinear model for a tropospheric duct.

21) Lang, R. H. (1978), Ray structure of ducted multipath for an LOS link, RADC-TR-78-123, May, Rome Air Development Center, Air Force Systems Command, Griffis Air Force Base, N.Y. 13441.

A propagation model for performing ray tracing in atmospheric ducts, as approximated by the tri-linear model.

22) Linfield, R. F., R. W. Hubbard and L. E. Pratt (1976), Transmission channel characterization by impulse response measurements, OT Report 76-96.

An impulse response measurement system is described where the resolution of multipath components is 6 ns.

23) Lundgren, C. W., and W. D. Rummler, Digital radio outage due to selective fading-observation vs. prediction from laboratory simulation, BSTJ, Vol. 58, No. 5, May-June, 1073-1100.

A statistical model for the three parameters:
1) f_o, the position of the fade minimum or notch and
2) b the amplitude of the multipath component in the channel transfer function, and
3) a multiplicative constant, a

The transfer function is

$$H(\omega) = a[1 - be^{-i(\omega-\omega_o)\tau}]$$

The statistics were gathered on an unprotected 26.4 mile hop in the 6-GHz band from Palmetto, Georgia to Atlanta, Georgia. The signal was modulated with an 8-PSK modem, typically with a pulse width τ = 6.3 ns. The modeled fading occurrences were scaled to the basis of a heavy fading month using the occurrence of time faded below a level at a single frequency as the means of calibration.

24) Neiburger, M. (1944), Temperature changes during formation and dissipation of West Coast stratus, J. Meteorol. 1., 29-41.

Neiburger noted in the Los Angles area that the base of the subsidence inversion layer undergoes marked changes in elevation, with a maximum about 8 am. and a minimum in the evening.

25) Ortenburger, L. N. (1979), Duct/SRLR, GTE Sylvania.

A comprehensive table of duct parameters such as trapping frequency, percent occurrence of layers, surface refractivity and gradients, layer thickness from many stations throughout the world.

26) Pappert, R., and C. Goodhart (1976), Waveguide calculations of signal levels in tropospheric ducting environments, NELC Tech. Note 3129, Feb., Naval Electronics Lab. Center, San Diego, Calif. 92152.

A theoretical model for calculating the fields in a tri-linear model for a tropospheric duct.

27) Ramadan, M. (1979), Availability prediction of 8 PSK digital microwave systems during multipath propagation, ICC conference proceedings.

A simple two ray model based on the 1971 Ruthroff model to study multipath.

28) Ringwalt, D. L., and F. C. Macdonald (1961), Elevated duct propagation in the tradewinds, IRE Trans. AP-9, 377-383.

Effects of tradewind inversion on propagation.

29) Rosenthal, J. (1972), Point Mugu forecasters handbook, Tech. Publication PMR-TP-72-1, Pacific Missile Range, Pt. Mugu, California 93042.

30) Rosenthal, J. (1973), PMR refractive support to Fleet Range Users in a highly refractive enviroment. Proc. Com. Third Fleets Navy Conf., Refractive Effects on EM Propagation, San Diego, California.

Rosenthal states that much of the coastal area of southern California, including the Pacific Missile Range, is usually in a moist marine layer capped by a rather strong and much drier inversion layer. The latter is strongly superrefractive and is almost always present, especially in the summer months.

31) Rummler, W. D. (1979), A new selective fading model: Application to propagation data, BSTJ, Vol. 58, No. 5, May-June, 1037-1071.

A three ray model for the channel transfer function;

$$H(\omega) = a[1 - be^{-i(\omega-\omega_o)\tau}]$$

The distribution of the parameter b is of the form $(1-b)^{2.3}$, the distribution of a is lognormal while the distribution for ω_o is constant at two different levels depending upon whether $\omega_o\tau$ is five times as likely to be less than $\pi/2$ than to be greater.

32) Ruthroff, C. L. (1971), Multiple-Path fading on line-of-sight microwave radio systems as a function of path length and frequency, BSTJ, Vol. 50, No. 7, Sept., 2375-2398.

Assuming the maximum phase difference between the direct and multipath rays to be $3\pi/4$ for a short path (i.e., just two rays rather than say 3 make up the received signal) corresponding to a difference in path length of $\Delta L = \frac{3}{8}\lambda$ or a maximum delay

$$\tau = \frac{3}{8f} \quad \text{seconds}$$

At a frequency of 20 GHz the maximum echo delay on a 5.5 km path is 0.01 875 ns. Pulses with a duration of one ns would suffer little degradation.

33) Starkey, B. J. (1956), Some aircraft measurements of beyond-the-horizon propagation phenomena at 91.3 Mc/s, Proc. IEEE 103B, 761-763.

Starkey studied the enhanced field strength and extended range related to extensive and persistent layers in the atmosphere.

34) Tattersall, R. L. O., and N. E. Cartwright (1977), Multipath propagation data collected from tests on line-of-sight radio paths at 11, 20 and 37 GHz during the period 1972-1975, Post Office Telecommunications, Research Dept. report No. 594 Feb., The Post Office Research Centre, Martlesham, Heath, Ipswich, U.K.

Data is presented for multipath fading during the period 1972-1975 on several terrestrial microwave radio links in the U.K. The fading was monitored on 8 experimental links in East Anglia with paths ranging from 4 to 22.8 km at frequencies close to 11, 20 and 37 GHz. Data were also collected from 6 geographically diverse 11 GHz communications links having path lengths of 14.4 to 36.2 km. The CD.'s generally show Rayleigh-type fading. The designed path clearances were made the same as those for Post Office operational communications radio-relay systems; i.e., a clearance of 0.577 of the radius of the first Fresnel-zone ellipsoid under an effective earths radius of 0.7. A ray-trace of the Purdown-Pen Hill path is shown in Figure B3 under normal atmospheric conditions and it would appear that the path is not LOS.

35) Thompson, M. C., L. E. Wood, H. B. Janes and D. Smith (1975), Phase and amplitude scintillations in the 10 to 40 GHz band, IEEE Trans. Ant. and Prop., Vol. AP-23, No. 6, Nov., 792-797

"Active" amplitude fading on a 64 km slant path at 19.1 and 25.4 GHz are shown in the time series in Figure B4. The correlation of the two signals was greater than 0.5 for lags greater than 5 sec.

36) Turner, D., B. J. Easterbrook and J. E. Golding (1966), Experimental investigation into radio propagation at 11.0-11.5 GHz, Proc. IEE, Vol. 113, No. 9, Sept., 1477-1489.

Fading statistics collected on 3 paths in U.K. due to multipath and precipitation.

37) Vigants, A. (1975), Space-Diversity Engineering, BSTJ, Vol. 54, No. 1, Jan., 103-142.

Space diversity was examined on 26 mile Atlanta-Palmetto, Georgia path at 4- and 6-GHz as an alternative form of protection against multipath fading.

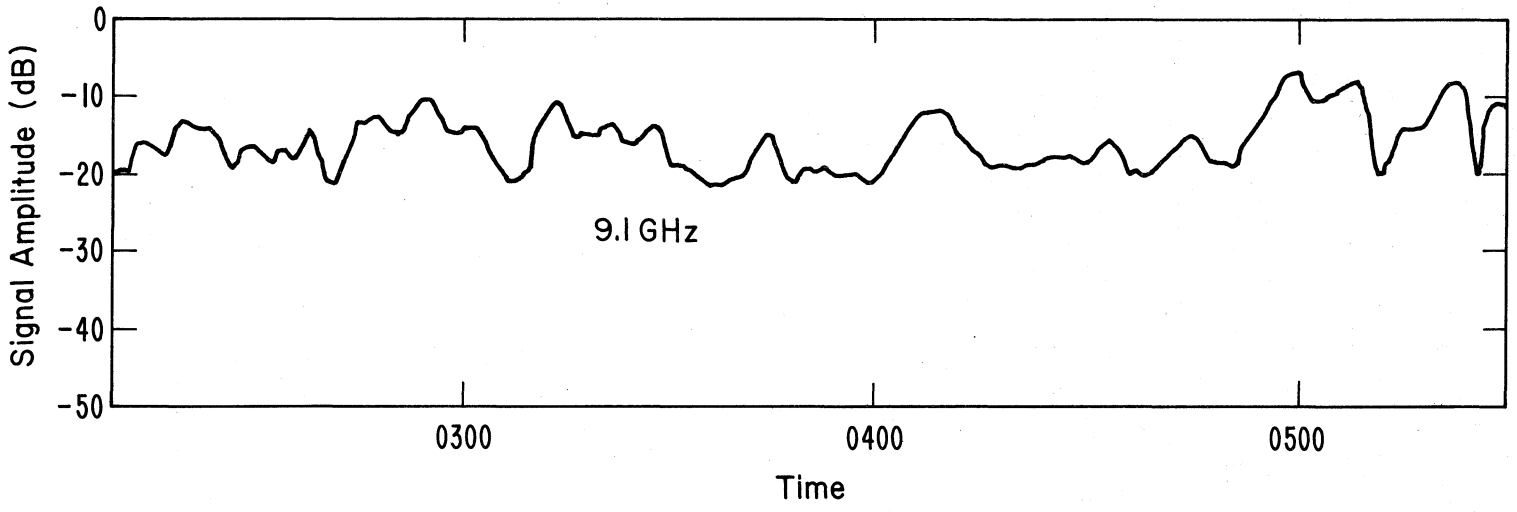

Figure B1. Time series for 9.1 GHz signal over 22.8 km path near Haswell in southeastern, Colorado, 3/8/66. $E\{9.1\ GHz\} \simeq -13\ dB^2$, $\sigma^2(9.1\ GHz) \simeq 126\ dB^2$. From Fig. 6, R. E. McGavin, H. T. Dougherty, C. B. Emmanual, Microwave Diversity Over Irregular Terrain, ESSA Tm, ERLTM-WPL3, December, 1968.

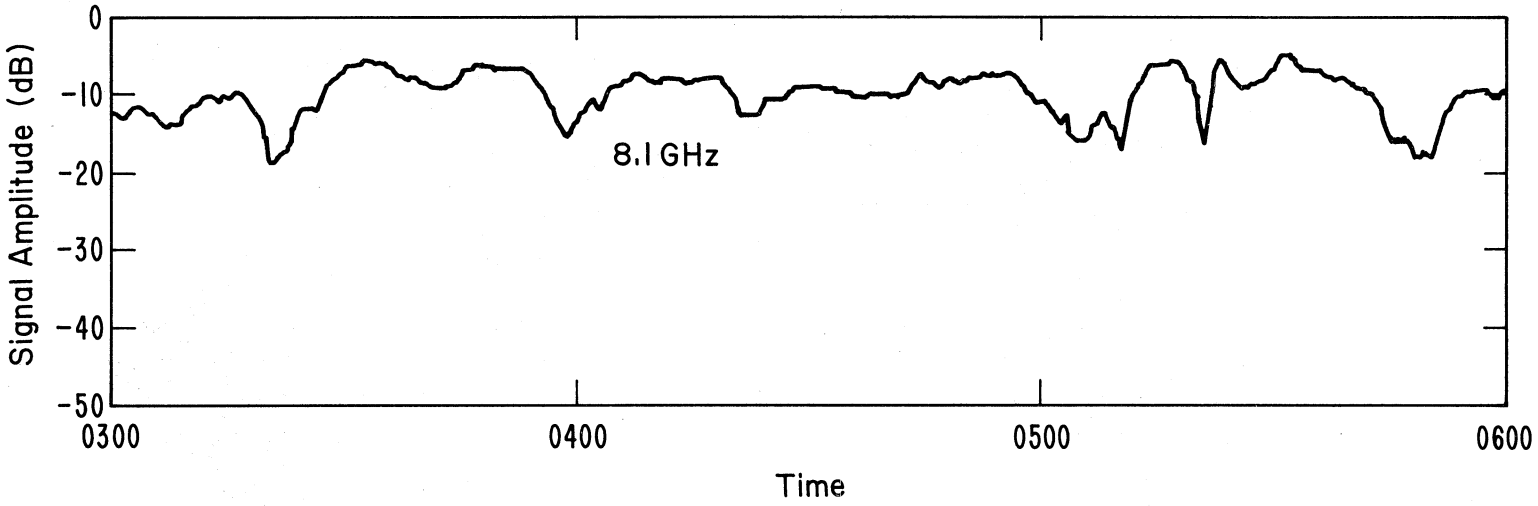

Figure B2. Time series for 8.1 GHz signal over 50 km Boone-Fowler path, 8/2/79. $E\{8.1\ GHz\} = -10$ dB. $\sigma^2(8.1\ GHz) \simeq 9\ dB^2$. From Fig. 7, W. J. Hartman, D. Smith (1975), Tilting antennas to reduce line-of-sight microwave link fading, Report No. FAA-RD-75-38, February, Prepared for U. S. Dept. of Transportation, FAA, Systems Research and Development Service, Washington, D. C. 20590.

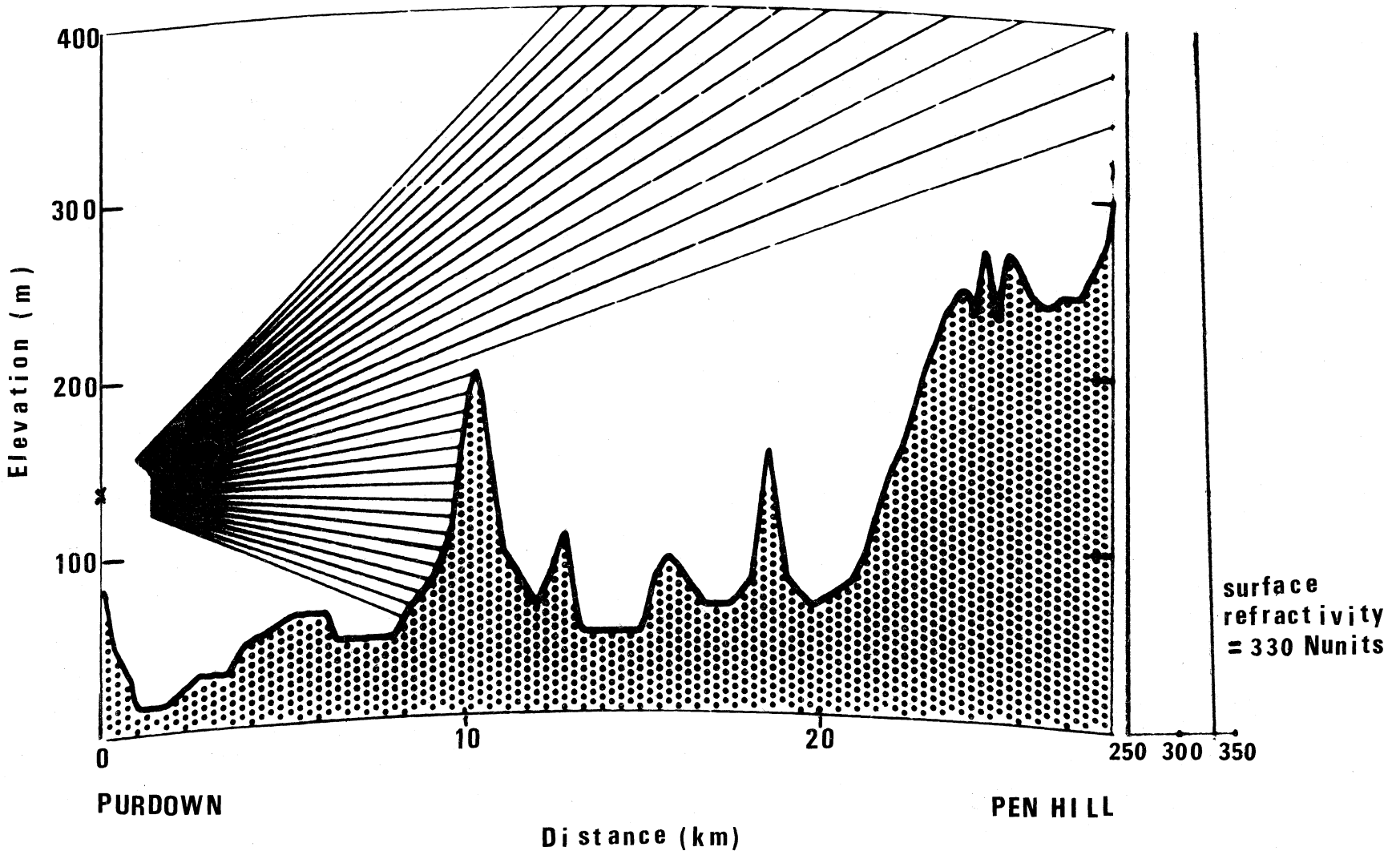

Figure B3. Ray trace for Purdown-Pen Hill path assuming a normal atmosphere with surface refractivity of 330 Nunits.

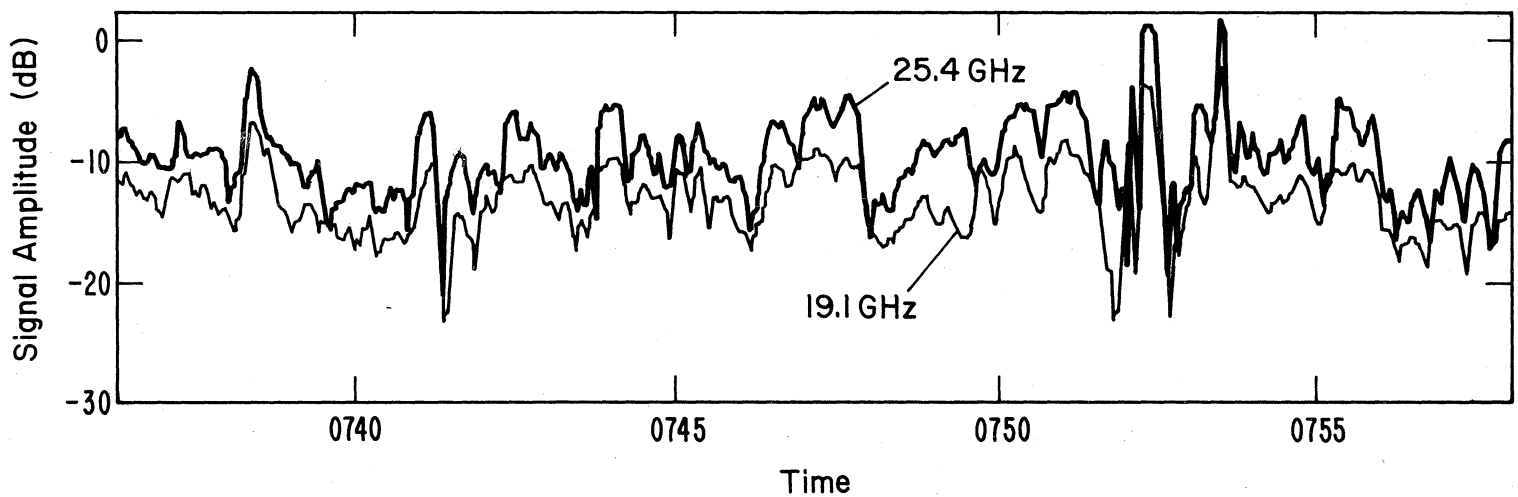

Figure B4. Time series for 19.1 and 25.4 GHz signals over 64 km path in Hawaii, 9/13/71. E{19.1 GHz} = -16 dB, σ^2(19.1 GHz) = 9 dB^2, E{25.4 GHz} = -12 dB, σ^2(25.4 GHz) = 11.5 dB^2. From Fig. 6, M. C. Thompson, Jr., Lockett E. Wood, Harris B. Janes, Dean Smith, (1975), Phase and Amplitude Scintillations in the 10 to 40 GHz Band, IEEE Trans. Ant. and Prop., Vol. AP-23, No. 6.

FORM OT-29
(3-73)

U.S. DEPARTMENT OF COMMERCE
OFFICE OF TELECOMMUNICATIONS

BIBLIOGRAPHIC DATA SHEET

	1. PUBLICATION OR REPORT NO. NTIA-Report-80-40	2. Gov't Accession No.
3. Recipient's Accession No.		

4. TITLE AND SUBTITLE

Fading Statistics on a 23 km Link at 9.6 and 28.8 GHz

5. Publication Date

June 1980

6. Performing Organization Code

NTIA/ITS

7. AUTHOR(S) R. H. Ott, K.C.Allen, E.J.Violette, R.H.Espeland, M.C.Thompson,Jr., and A. R. Mitz

9. Project/Task/Work Unit No.

8. PERFORMING ORGANIZATION NAME AND ADDRESS

U. S. Department of Commerce
National Telecommunications and Information Administration
Institute for Telecommunication Sciences
Boulder, Colorado 80303

10. Contract/Grant No.

11. Sponsoring Organization Name and Address

Same

12. Type of Report and Period Covered

13.

14. SUPPLEMENTARY NOTES

15. ABSTRACT *(A 200-word or less factual summary of most significant information. If document includes a significant bibliography or literature survey, mention it here.)*

An experimental study of atmospheric multipath on a 23 km link at 9.6 and 28.8 GHz near Boulder, Colorado, is described. The preliminary observations were made for three days in July 1979 when a strong inversion layer was present, creating an elevated tropospheric duct. The possible influence of antenna aperture size on atmospheric multipath was investigated by observing fades and enhancements on the 28.8 GHz carrier using a 10° horn and a 1.2° parabolic dish. Continuous height-gain observations were obtained using the 300 m. tower at Erie, Colorado, as one end of the link. Meteorological data at the tower were also recorded during observation periods of the radio signal.

16. Key words *(Alphabetical order, separated by semicolons)*

Atmospheric multipath, fading, micromillimeter wave, refractivity structure.

17. AVAILABILITY STATEMENT

☒ UNLIMITED.

☐ FOR OFFICE DISTRIBUTION.

18. Security Class *(This report)*

Unclassified

20. Number of pages

50

19. Security Class *(This page)*

Unclassified

21. Price:

☆U.S. GOVERNMENT PRINTING OFFICE: 1980-0-678-845/458

USCOMM-DC 29716-P73
USCOMM - ERL